Heliyon 10 (2024) e27615

Contents lists available at ScienceDirect

Heliyon

journal homepage: www.cell.com/heliyon

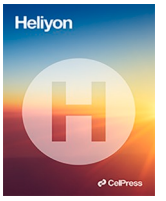

Research article

Distributionally robust optimization scheduling of port energy system considering hydrogen production and ammonia synthesis

Xiaoou Liu

China Power Engineering Consulting Group CO.,LTD., Ande Road 65, Xicheng District, Beijing, 100120, China

ARTICLE INFO

Keywords:
Port energy system
Green hydrogen
Ammonia synthesis
Wasserstein distance
Distributionally robust optimization

ABSTRACT

In order to effectively address the uncertainty risks of port energy system caused by intermittence and fluctuation of renewable energy, this paper proposes a scheduling method for port energy system based on distributionally robust optimization (DRO) considering ammonia synthesis after hydrogen production by water electrolysis (P2H2A), and uses real data from Tianjin Port for example analysis. The calculation results show that 1 h selected for the scheduling interval of P2H2A is reasonable, it can ensure that the ammonia synthesis reaction transitions smoothly to the new steady state, and the temperature and pressure of the ammonia converter meet safety constraints. The two-stage scheduling of port energy system based on DRO can be divided into pre-scheduling in the day-ahead stage and rescheduling in the intraday stage, which can improve the capacity of anti-risk for stochastic optimization and overcome the conservatism of robust optimization, and consider economy and robustness. Moreover, the rescheduling decision can be transformed to a prediction error function, the result of two-stage scheduling based on DRO is the pre-scheduling result, which is between the cost of stochastic optimization and robust optimization. As the Wasserstein distance-based sphere radius increases, the pre-scheduling cost of DRO gradually deviates from risk neutral stochastic optimization and leans towards risk averse robust optimization. When the Wasserstein distance-based sphere radius remains constant, the variance gradually decreases as the number of scenarios increases, which can promote the Wasserstein distance-based fuzzy set to converge to the true distribution. When the number of scenarios is greater than 15, the pre-scheduling cost will no longer fluctuate significantly, and the calculation time is in the range of 1200 s–6600 s. It can meet the demands of day-ahead scheduling calculation time. Therefore, the scheduling model has outstanding advantages in the computing time to improve the flexibility and economy of Tianjin Port's energy system scheduling, considering ammonia synthesis after hydrogen production using renewable energy.

1. Introduction

Ports undertake 80% of global transportation tasks, and produce 3%–5% of global CO_2, 14%–15% of NO_X and SO_X [1], which will cause adverse impacts on the environment. Under the goal of emission peak and carbon neutrality, China is accelerating the construction of green and low-carbon ports, promoting port electrification reconstruction, and gradually replacing fossil fuels with renewable clean energy source [2]. Taking Tianjin Port as an example, as an important foreign trade port in Tianjin, it has speeded up their strategy to construct ecological coastline and green port in recent years. Tianjin Port attaches great importance to the

E-mail address: liuxiaoou126@126.com.

https://doi.org/10.1016/j.heliyon.2024.e27615
Received 25 July 2023; Received in revised form 18 January 2024; Accepted 4 March 2024
Available online 5 March 2024

Nomenclature

P_t^{P2H}	the power consumption of P2H at time t
$P^{P2H,0}$	the power of auxiliary equipment
c^{P2H}	the power coefficient of electrolyzers
$Q_t^{H_2}$	the hydrogen production volume at time t
$r_{\max}^{P2H}$	the upper limit of ramp rate for P2H
$Q_t^{NH_3}$	the ammonia production volume at time t
$Q_{\max}^{NH_3}$, $Q_{\min}^{NH_3}$	the upper and lower limits of ammonia production volume
$r_{\max}^{NH_3}$, $r_{\min}^{NH_3}$	the upper and lower limit of ramp rate for ammonia synthesis
$P^{NH_3,0}$	the fixed power of ammonia production
c^{NH_3}	the constant coefficient of ammonia production
$Q_t^{H_2,out}$	the outlet flow rate of HST
η^{HST}	the efficiency of hydrogen storage/release for HST
VOL^{HST}	the installed capacity of HST
$S_{\max}^{HST}$, $S_{\min}^{HST}$	the upper and lower limits of SOC for HST
$Q_{\max}^{H_2}$	the upper limit of the flow for HST
M_{H_2}	the molar mass of hydrogen
η_c	the compressor efficiency
Q_t^{Air}	the air flow rate at time t
M_{Air}	the molar mass of air
S_t^{HES}	the SOC of HES at time t
$H_t^{HES,ch}$, $H_t^{HES,dis}$	the power of heat storage/release for HES at time t
η^{HES}	the heat storage/release efficiency for HES
VOL^{HES}	the installed capacity of HES
$S_{\max}^{HES}$, $S_{\min}^{HES}$	the upper and lower limits of SOC for HES
$H_{\max}^{HES}$	the upper limit of power for HES
L_t^{EC}	the cooling power of the EC at time t
P_t^{EC}	the electrical power of EC at time t
η^{EC}	the efficiency of EC
$L_{\max}^{EC}$	the upper limit of the cooling power for EC
L_t^{AC}	cooling power of the AC at time t
P_t^{AC}	the electrical power of AC at time t
η^{AC}	the efficiency of AC
$L_{\max}^{AC}$	the upper limit of the cooling power for AC
H_t^{GB}	the thermal power of the GB at time t
G_t^{GB}	the gas consumption of GB at time t
η^{GB}	the efficiency of GB
$H_{\max}^{GB}$	the upper limit of the thermal power for GB
P_t^{GT}, H_t^{GT}	the electrical power and thermal power of the GT at time t
$\eta^{GT,p}$, $\eta^{GT,h}$	the efficiency of electric power and heat generation for GT
$P_{\max}^{GT}$, $P_{\min}^{GT}$	the upper and lower limits of the electrical power for GT
$r_{\max}^{GT}$	the upper limit of the ramp rate for GT
U_t^{GT}	the on/off status of GT at time t
$T_{\min}^{GT}$	the lower limit of the time span of start and stop for GT
$\mathbf{c}^{\mathrm{T}}$	the coefficient vector of the pre-scheduling decision variable x
X	the set of pre-scheduling decision variables x
$\mathbf{P}_{\mathrm{e,inj}}$	N_e-dimensional nodal injection power column vector
sup(·)	the supremum function
D	the true distribution of prediction errors
$\mathscr{U}$	a fuzzy set
$\boldsymbol{\omega}^u$	the prediction error of renewable energy power generation
$Q(\boldsymbol{x},\boldsymbol{\omega}^u)$	the rescheduling cost
A	the coefficient matrix of the constraint conditions in the pre-scheduling stage
b	the parameter vector of the constraint conditions in the pre-scheduling stage
$E_D(\cdot)$	mathematics expectation

$\boldsymbol{y}(\boldsymbol{x},\boldsymbol{\omega}^u)$	the decision variable in the rescheduling stage
$\mathbf{d}^{\mathrm{T}}$	the coefficient vector
$\mathbf{Z}$	the coefficient matrix of the constraint conditions in the rescheduling stage
$g(\boldsymbol{\omega}^u)$	the parameter vector
$\mathrm{D_e}$	the empirical distribution
L(Ξ)	all probability distributions in support set Ξ
M	the uncertain variables
α	the confidence level
μ^{ti}	the average value of the sample data
ω_m^u	the m-th uncertainty parameter
Γ^{ti}	the variance of the sample data
ω_m^{ti}	the m-th sample data
θ_m^u	the m-th element of θ^u
l	the boundary of θ_m^u
$\mathrm{l_{max}}$	the maximum of l
$\mathrm{p}^{\mathrm{std}}$, $\not{\mathrm{e}}^{std}$	the probability distribution and fuzzy set of uncertain parameters
C_t^{main}	the energy purchase and sale cost
C_t^{CO2}	the carbon emission cost
C_t^{vary}	the fluctuation penalty cost
c^{pr,NH_3}	the sale price of ammonia
$c_t^{pr,e,s}$, P_t^{sell}	the price and quantity that port sells electricity to municipal power grid
$c_t^{pr,e,b}$, P_t^{buy}	the price and quantity that port purchases electricity from municipal power grid
$c_t^{pr,g}$	the price of nature gas
$c^{pr,CO2}$	the carbon price
$\delta^{g,CO2}$, $\delta^{p,CO2}$	the carbon emissions factors of nature gas and municipal power grid
c^{vary}	the power fluctuation penalty coefficient of municipal power grid
P_t^{vary}	the power fluctuation of municipal power grid caused by renewable energy
$\widetilde{Q}_t^{NH_3}$	the adjustment value of ammonia production volume at time t
$\widetilde{P}_t^{sell}$, $\widetilde{P}_t^{buy}$	the adjustment value of the quantity that port sells electricity to municipal power grid, and port purchases electricity from municipal power grid
$\widetilde{G}_t^{GT}$, $\widetilde{G}_t^{GB}$	the adjustment values for gas consumption of gas turbine and gas fired boiler
$c^{pr,re}$, $c^{pr,load}$	the penalty coefficients for the power curtailment of renewable energy power generation and load shedding
$P_t^{cut,wt}$, $P_t^{cut,pv}$, $P_t^{cut,load}$	the quantity for the power curtailment of wind turbine, photovoltaic and load shedding
$P_{\max}^{MPG}$	the upper limit of exchange power between port and municipal power grid
P_t^{WT}, P_t^{PV}	the power of wind turbine and photovoltaic
$P_t^{load,e}$, $H_t^{load,h}$, $L_t^{load,c}$	the electric load, heating load, and cooling load at time t
$P_t^{cut,i}$, $P_t^{cut,load}$	the reduction of renewable energy power generation and load
ω^u	the prediction error of renewable energy power generation
$\boldsymbol{T}_k^{cc}$	Opening or closing instructions for branches in power/heat/gas system and energy station

comprehensive recovery and utilization of oilfield associated gas, actively implements the "from coal to gas" and "from oil to gas" projects, and has achieved significant environmental protection efforts. By building rooftop photovoltaic (PV) and offshore wind turbine (WT), Tianjin Port builds a integrate energy system wherein renewable energy constitutes the main body of energy, supplemented by natural gas distributed energy system, and coordinated with municipal power grid (MPD), in order to optimize the synthetical efficiency for low-carbon energy utilization.

However, enhancing the capacity of the large-scale renewable energy source utilization requires the dispatching of a large amount of diversified flexibility resources in ports [3]. Since the renewable energy have the intrinsic intermittence and fluctuation, their integration into the port will present a great challenge on the operating reliability of port energy system [4]. Therefore, the rational integration of diversified flexibility resources in ports, the optimal scheduling of port energy systems, and the improvement of anti-risk ability have become a key problem to be solved urgently.

1.1. Deficiency of current research

In the context of emission peak and carbon neutrality, as a low-carbon and clean secondary energy, hydrogen energy is a green energy carrier that can enhance the capacity of renewable energy utilization and promote the low-carbon transition of port energy system. Hydrogen is an industrial raw material for synthesizing ammonia, which is one of the main methods for the large-scale consumption of green hydrogen [5]. Demonstration projects have realized the commissioning and operation [6], and the number

of projects initiated has rapidly increased in the world [7]. That can in turn create a larger install base of renewable energy power generation and hydrogen production by electrolysis. Using green hydrogen instead of gray hydrogen as feed gas in the ammonia synthesis, accelerating the renewable energy base construction of the green port and hydrogen city, both have become an important development direction for carbon emission reduction in Chinese ports [8]. In the long run, realizing green production and increasing productivity of synthetic ammonia will help reduce industry trade deficit.

Therefore, the ammonia synthesis after hydrogen production using renewable energy is expected to provide a large amount of flexible resources for the port energy system. It should adjust to the intermittence and fluctuation of renewable energy power generation, and has the ability to be the flexible and adjustable load [9,10]. With the technology development and engineering construction of green hydrogen, the technology of power to hydrogen (P2H) and ammonia synthesis after hydrogen production by water electrolysis (P2H2A) have become research hotspots. The current research on the load regulation characteristics of P2H mainly focuses on technical and economic aspects [11], scheduling control [12], and operation modes [13]. Compared with P2H, the research on flexible regulation characteristic of P2H2A is relatively limited. A joint scheduling model is proposed based on historical electricity prices [14], considering electricity, hydrogen and ammonia. An optimized scheduling method is proposed for ammonia synthesis after Hydrogen production using wind power [15], focusing on analyzing the impact of the sitting and sizing on the operating costs of ammonia plant. An energy management strategy is proposed for industrial parks about the integrated utilization of electricity, hydrogen and ammonia [16]. A P2H2A optimization scheduling model is proposed based on day-ahead electricity price forecasting [17], in order to evaluate the impact of parameter variation of synthetic ammonia on revenue. However, the above references were deterministic optimization methods based on the forecasting of electricity prices or renewable energy, less related to the schedulability analysis of P2H2A under uncertainty. Although hydrogen storage tank can be installed between the hydrogen production and ammonia synthesis sections to suppress hydrogen flow fluctuation, the capacity of hydrogen storage tank is limited by investment costs and safety constraints. Therefore, it is necessary to study the potentiality analytical methods for P2H2A to be the flexible and adjustable load, in order to provide a quantitative reference for P2H2A taking in renewable energy utilization and the implementation of power demand balance.

The port can achieve the large-scale transmission, grid-connected, and utilization of offshore renewable energy power generation. Therefore, offshore renewable energy power generation integration to the port with high penetration will present a great uncertainty risk, which cannot be ignored. At present, the analysis methods for uncertainty problems in power-gas coupled system include stochastic optimization [18], and robust optimization [19,20]. As the number of scenarios increases, stochastic optimization methods may cause dimension disaster, and lead to computational difficulties. Due to the low probability of the worst-case scenario occurring, the robust optimization results are too conservative. In order to overcome the limitations and shortcomings of the above two methods, researches are committed to the research of distributionally robust optimization (DRO) methods [21]. DRO can generate a fuzzy set containing all probability distributions based on sample data of uncertain variables. Under the scenario where the prediction error of uncertain variable follows the worst-case probability distribution in a fuzzy set, the scheduling strategy can be determined. Compared with stochastic optimization, DRO has stronger robustness, and it does not need to the accurate distributed function of uncertain variables during calculation [22]. DRO considers the probability distribution information of uncertain variables to avoid overly conservative scheduling strategy [23]. DRO has been applied in other fields [24,25], but there is relatively little research on it for port energy systems. Therefore, it is necessary to conduct research on optimal dispatch of port energy system with DRO in response to the uncertainty of offshore renewable energy power generation.

1.2. Structure of thesis

In summary, the hydrogen energy is a green energy carrier that can enhance the capacity of renewable energy utilization and promote the low-carbon transition of port energy system, and is an important industrial raw material for synthesizing ammonia. It can be expected to participate in the scheduling of port energy system as flexible resources. Therefore, it is necessary to study the potentiality analytical methods for P2H2A to be the flexible and adjustable load, in order to provide a quantitative reference for P2H2A taking in renewable energy utilization and the implementation of power demand balance. In order to overcome the limitations and shortcomings of stochastic optimal dispatch and robust optimal dispatch, the DRO is necessary to be used in optimal dispatch of port energy system with the property of renewable energy uncertainty.

To make up the existing research insufficiency, this paper proposes a scheduling method for port energy system based on distributionally robust optimization considering ammonia synthesis after hydrogen production using renewable energy, and uses real data from Tianjin Port for example analysis. Firstly, to describe the capability of load regulation for ammonia synthesis after hydrogen production by water electrolysis (P2H2A), an overall architecture model of P2H2A was constructed in Part II. The model of P2H2A considers the safety constraints of hydrogen production and ammonia synthesis chemical processes, which can make P2H2A serve as a flexible resource for distributionally robust optimization scheduling of port energy systems while ensuring safety. Secondly, the Wasserstein distance is used to characterize the uncertain fuzzy set in Part III, which is consist of the probability distribution of renewable energy power generation. By fitting the probability distribution of prediction error of renewable energy power generation, various scenarios of its output interval under different confidence levels can be obtained. Thirdly, for the port energy system with P2H2A, DRO is used to build a two-stage scheduling model considering Wasserstein distance-based fuzzy set in Part IV. The model can be converted into a mixed integer linear programming model for being easy to solve by using the strong duality theorem. Finally, example analysis is conducted based on the real data of Tianjin Port in Part V. The results show that P2H2A can significantly reduce the carbon emission and improve the flexibility for the port energy system. The proposed model not only considers the economy of the port energy system, but also further ensures the capability of anti-risk and robustness under the uncertainty of renewable energy power

generation.

1.3. Main innovation of paper

This paper proposes a scheduling method for port energy system based on distributionally robust optimization considering hydrogen production and ammonia synthesis, and the main innovations are as follows.

(1) A low-carbon energy architecture of port is established, which may be divided into three structural layers, such as the energy input layer, energy conversion and storage layer, and energy output layer. The system structure of ammonia synthesis after hydrogen production by water electrolysis is proposed, which can participate the operation of port energy system as low-carbon and flexible resources.
(2) The model of the ammonia synthesis section has been reasonably simplified. The scheduling model for P2H2A is presented, which can make P2H2A adapt to the uncertain of renewable energy power generation. It can help to settle the accommodation problem of large-scale renewable energy power generation, and improve the economy and flexibility of energy system in the port.
(3) Considering the risks brought by the uncertainty of renewable energy power generation, the Wasserstein distance is used to characterize the uncertain fuzzy set of uncertainty parameter prediction errors. The Wasserstein distance-based fuzzy set independent of prior knowledge is data-driven, and can make the DRO model has good operation ability, and can be less conservative.
(4) DRO is used to build a two-stage scheduling model of port energy system. The scheduling strategy based on DRO may enhance the anti-risk ability of scheme, and avoid the impact of overly conservative on the scheme economic at the same time. The strong duality theorem is used to reconstruct the model, which is equivalent to the mixed integer linear programming problem, in order to make the problem easy to solve.

2. Port energy system structure and model

Vigorously developing new energy, mainly wind power and photovoltaic, is the necessary path for port energy saving and emission reduction. As a low-carbon and clean secondary energy source, hydrogen energy is a green energy carrier that can increase the capacity of renewable energy utilization and promote low-carbon transition of port energy structure. Hydrogen is an industrial raw material for synthesizing ammonia, which is one of the main methods for the large-scale consumption of green hydrogen. Tianjin Port has the conditions to build a green energy hub with ammonia and hydrogen. Therefore, it is planned to build an integrated energy system in the port, mainly based on renewable energy power generation, supplemented by natural gas distributed energy system, and coordinated with municipal power grid.

The energy structure of port is shown in Fig. 1. The energy input layer includes photovoltaic (PV), wind turbine (WT), municipal power grid (MPD), natural gas source, etc. The energy conversion and storage layer includes ammonia synthesis after hydrogen production by water electrolysis (P2H2A), electric cooler (EC), absorption cooler (AC), gas turbine (GT), gas fired boiler (GB), heat energy storage device (HES), etc. P2H2A consists of an electrolyzer, N_2 production via air separation (AS), hydrogen storage tank (HST), and ammonia converter. The energy output layer includes electric/cooling/heating load and liquid ammonia. Energy conversion equipment can achieve reliable supply of energy demand and improve energy efficiency through multi-energy complementary

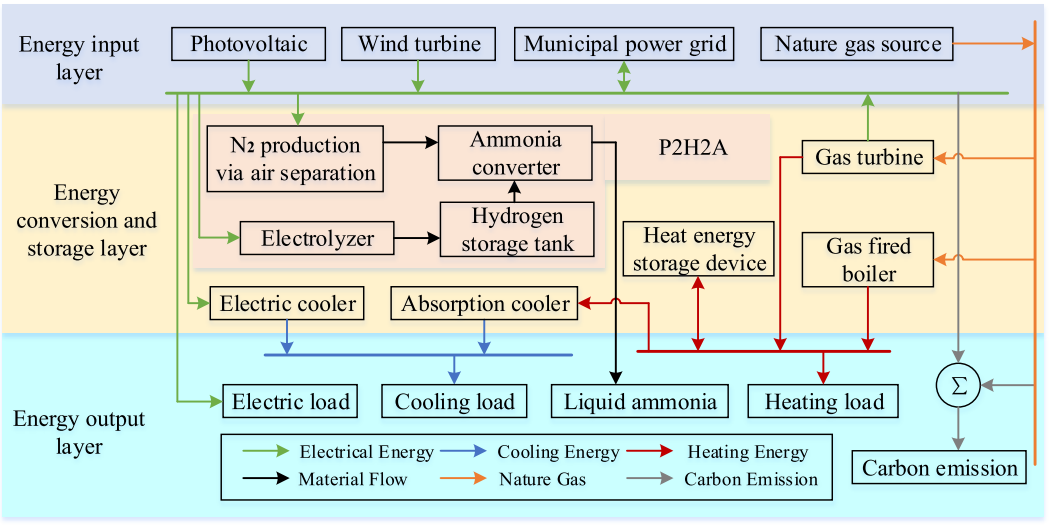

Fig. 1. Energy structure of port.

mode. P2H2A can not only improve the capacity of renewable energy utilization, but also bring considerable economic benefits to the port. HES and GB can achieve decoupling heat-power of GT, the peak regulating capacity of GT can be increased. HST can achieve energy transfer for long time scales, and are suitable for stabilizing the daily, weekly, and even seasonal electricity fluctuations. Therefore, it is necessary to build a low-carbon, clean energy system to promote the sustainable development of port.

2.1. Modeling of ammonia synthesis after hydrogen production by water electrolysis

Ammonia synthesis after hydrogen production using renewable energy is a deep coupling between power system and chemical system, has the ability to adjust their energy demand to the fluctuation of renewable energy. It involves the complex regulation process of safe, robust and coordination for multiple systems of renewable energy power generation, hydrogen production and ammonia synthesis. The technology of alkaline water electrolysis is usually used in the P2H, which has the advantages of mature state of art, lower cost and long life. The ammonia synthesis section usually adopts the Harbor-Bosch process [26], which is consist of ammonia converter, ammonia separation, circulation recovery, etc. The principle of ammonia synthesis is shown in Eq. (1). The reaction principle of P2H2A is shown in Fig. 2.

$$N_2(g) + 3H_2(g) \rightarrow 2NH_3(g) \tag{1}$$

The overall process of P2H2A is shown in Fig. 2. T and p represent the temperature and pressure of each stage, respectively. H_2 and N_2 are respectively produced by the P2H section and the air separation section. The ammonia synthesis section is an exothermic reaction. The ammonia converter operates in a high-temperature and high-pressure environment to ensure catalyst activity and reaction rate. The raw gas needs to be pressurized through multi-stage compression, and heat exchanged with the high-temperature mixed gas at the outlet of ammonia converter to increase the gas temperature. After the reaction is completed, liquid ammonia products can be obtained from the mixed gas after heat exchange, cooling, and ammonia separation section. The unreacted raw gas will be recompressed and recycled back into the ammonia converter to continue the reaction.

2.1.1. P2H model

The power of P2H usually includes the power of electrolyzers and the power of auxiliary equipment [27]. The load rate of a single electrolyzer is about 20%–100%. Through the strategy combination of unit startup and shutdown and load distribution, the load rate of multiple electrolyzers can continuously change within the range of 5%–100% [27], and the energy conversion efficiency is close to linear. Therefore, the linear function between power consumption and hydrogen production volume for P2H section is shown in Eq. (2).

$$0 \le P_t^{P2H} = P^{P2H,0} + c^{P2H} Q_t^{H_2} \le P_{\max}^{P2H} \tag{2}$$

$$-r_{\max}^{P2H} \le P_t^{P2H} - P_{t-1}^{P2H} \le r_{\max}^{P2H} \tag{3}$$

In formula, P_t^{P2H} is the power consumption of P2H at time t. $P_{\max}^{P2H}$ is the upper limit of P2H power. $P^{P2H,0}$ is the power of auxiliary equipment, which is taken as 0.9% of $P_{\max}^{P2H}$. c^{P2H} is the power coefficient of electrolyzers, taken as 0.0048 MWh/Nm^3. $Q_t^{H_2}$ is the hydrogen production volume at time t. $r_{\max}^{P2H}$ is the upper limit of ramp rate for P2H [28], taken as 50% × $P_{\max}^{P2H}$ per minute.

2.1.2. Ammonia synthesis model

The ammonia synthesis section can adjust the ammonia production volume to the fluctuation of hydrogen flow. Due to constraints such as thermal equilibrium and catalyst activity [29], the ammonia production volume should be maintained within a given range, as shown in Eq. (4). Ammonia separation, circulation recovery, compression, and other processes all need power consumption. The linear function between power consumption $P_t^{NH_3}$ and ammonia production volume for ammonia synthesis section is shown in Eq. (6).

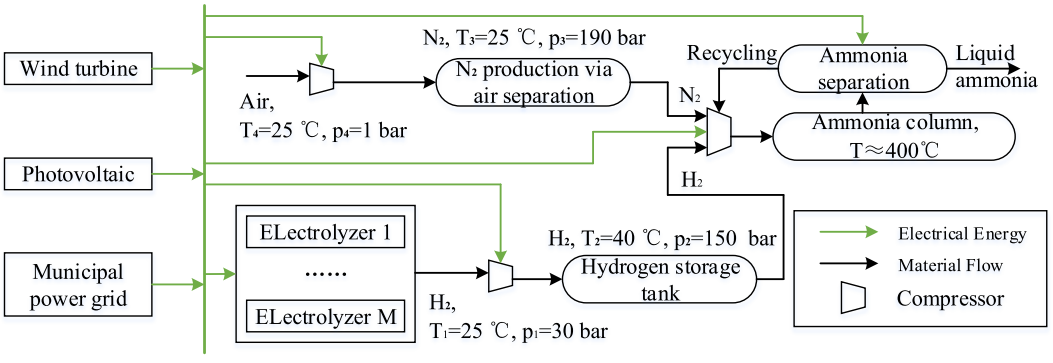

Fig. 2. Reaction principle of ammonia synthesis after hydrogen production by water electrolysis.

$$Q_{\min}^{NH_3} \le Q_t^{NH_3} = Q_{t-1}^{NH_3} + r_t^{NH_3} \le Q_{\max}^{NH_3} \tag{4}$$

$$r_{\min}^{NH_3} \le r_t^{NH_3} \le r_{\max}^{NH_3} \tag{5}$$

$$P_t^{NH_3} = P^{NH_3,0} + c^{NH_3} Q_t^{NH_3} \tag{6}$$

In formula, $Q_t^{NH_3}$ is the ammonia production volume at time t. $Q_{\max}^{NH_3}$ and $Q_{\min}^{NH_3}$ are the upper and lower limits of ammonia production volume, $Q_{\min}^{NH_3}$ is taken as 20% of $Q_{\max}^{NH_3}$. $r_{\max}^{NH_3}$ and $r_{\min}^{NH_3}$ are is the upper and lower limit of ramp rate for ammonia synthesis, which are taken as 15% and −25% of $Q_{\max}^{NH_3}$ respectively. $P^{NH_3,0}$ is fixed power. c^{NH_3} is a constant coefficient.

2.1.3. N_2 production and storage equipment model

Due to fluctuations in renewable energy power generation, there is fluctuation in hydrogen production volume. The fluctuation of hydrogen flow can be smoothly adjusted by hydrogen storage tank (HST), in order to meet the stability requirements of hydrogen flow used in ammonia synthesis. The state of charge (SOC) for HST S_t^{HST} and the power of the hydrogen compressor $P_t^{H_2,C}$ are shown in Eqs. (7)–(9) [30].

$$S_t^{HST} = S_{t-1}^{HST} + \left(Q_t^{H_2}\eta^{HST} - Q_t^{H_2,out} / \eta^{HST}\right) / VOL^{HST} \tag{7}$$

$$S_{\min}^{HST} \le S_t^{HST} \le S_{\max}^{HST}, \quad 0 \le Q_t^{H_2}, Q_t^{H_2,out} \le Q_{\max}^{H_2} \tag{8}$$

$$P_t^{H_2,C} = \left[\left(Q_t^{H_2} / M_{H_2}\right) RT_1 \ln(p_2 / p_1)\right] / \eta_c \tag{9}$$

In formula, $Q_t^{H_2,out}$ is the outlet flow rate of HST. η^{HST} is the efficiency of hydrogen storage/release for HST. VOL^{HST} is the installed capacity of HST. $S_{\max}^{HST}$ and $S_{\min}^{HST}$ are the upper and lower limits of SOC for HST, respectively. $Q_{\max}^{H_2}$ is the upper limit of the flow for HST. M_{H_2} is the molar mass of hydrogen. R is the ideal gas constant. η_c is the compressor efficiency, which is taken as 60%.

In addition, the N_2 required for ammonia synthesis can be obtained through air separation (AS). The process requires multi-stage compressors to gradually pressurize the air from atmospheric pressure, and the power consumption is shown in Eq. (10).

$$P_t^{AS} = \left[\left(Q_t^{Air} / M_{Air}\right) RT_4 \ln(p_3 / p_4)\right] / \eta_c \tag{10}$$

In formula, Q_t^{Air} is the air flow rate at time t. M_{Air} is the molar mass of air.

Compared to P2H, the power consumption of hydrogen storage and N_2 production processes is smaller. Compared with the power consumption of P2H2A, the power consumption changes caused by temperature and pressure changes in Eqs. (9) and (10) can be approximately ignored. For simplicity, this paper assumes that temperatures T_1, T_4, and pressures p_1, p_2, p_3, and p_4 are constant.

According to the mass balance relationship of the ammonia synthesis reaction, the relationship between the ammonia production volume $Q_t^{NH_3}$ and the outlet flow rate of HST $Q_t^{H_2,out}$ is shown in Eq. (11).

$$Q_t^{NH_3} = 2Q_t^{H_2,out}/3 \tag{11}$$

Considering that heat energy storage (HES) device is similar to HST, the model of HES is briefly described as follows.

$$S_t^{HES} = S_{t-1}^{HES} + \left(H_t^{HES,ch}\eta^{HES} - H_t^{HES,dis} / \eta^{HES}\right) / VOL^{HES} \tag{12}$$

$$S_{\min}^{HES} \le S_t^{HES} \le S_{\max}^{HES}, \quad 0 \le H_t^{HES,ch}, H_t^{HES,dis} \le H_{\max}^{HES} \tag{13}$$

In formula, S_t^{HES} represents the SOC of HES at time t. $H_t^{HES,ch}$ and $H_t^{HES,dis}$ respectively represent the power of heat storage/release for HES at time t. η^{HES} is heat storage/release efficiency for HES. VOL^{HES} is the installed capacity of HES. $S_{\max}^{HES}$ and $S_{\min}^{HES}$ are the upper and lower limits of SOC for HES. $H_{\max}^{HES}$ is the upper limit of power for HES.

2.2. Modeling of cooling and heating equipment

2.2.1. Electric cooler

$$0 \le L_t^{EC} = P_t^{EC}\eta^{EC} \le L_{\max}^{EC} \tag{14}$$

In formula, L_t^{EC} is the cooling power of the electric cooler (EC) at time t. P_t^{EC} is the electrical power of EC at time t. η^{EC} is the efficiency of EC. $L_{\max}^{EC}$ is the upper limit of the cooling power for EC.

2.2.2. Absorption cooler

$$0 \le L_t^{AC} = P_t^{AC}\eta^{AC} \le L_{\max}^{AC} \tag{15}$$

In formula, L_t^{AC} is the cooling power of the absorption cooler (AC) at time t. P_t^{AC} is the electrical power of AC at time t. η^{AC} is the efficiency of AC. $L_{\max}^{AC}$ is the upper limit of the cooling power for AC.

2.2.3. Gas fired boiler

$$0 \le H_t^{GB} = G_t^{GB}\eta^{GB} \le H_{\max}^{GB} \tag{16}$$

In formula, H_t^{GB} is the thermal power of the gas fired boiler (GB) at time t. G_t^{GB} is the gas consumption of GB at time t. η^{GB} is the efficiency of GB. $H_{\max}^{GB}$ is the upper limit of the thermal power for GB.

2.2.4. Gas turbine

$$P_{\min}^{GT} \le P_t^{GT} = G_t^{GT}\eta^{GT,p} \le P_{\max}^{GT} \tag{17}$$

$$H_t^{GT} = G_t^{GT}\eta^{GT,h} \tag{18}$$

$$-r_{\max}^{GT} \le P_t^{GT} - P_{t-1}^{GT} \le r_{\max}^{GT} \tag{19}$$

$$U_t^{GT} - U_{t-1}^{GT} \le U_\tau^{GT} \le 1 + U_t^{GT} - U_{t-1}^{GT}, \quad \tau \in \left[t+1, t+T_{\min}^{GT} - 1\right] \tag{20}$$

In formula, P_t^{GT} and H_t^{GT} are the electrical power and thermal power of the gas turbine (GT) at time t. $\eta^{GT,p}$ and $\eta^{GT,h}$ respectively refer to the efficiency of electric power and heat generation for GT. $P_{\max}^{GT}$ and $P_{\min}^{GT}$ are the upper and lower limits of the electrical power for GT. $r_{\max}^{GT}$ is the upper limit of the ramp rate for GT. U_t^{GT} indicates the on/off status of GT at time t. $U_t^{GT} = 1$ means that GT is operation, $U_t^{GT} = 0$ means that GT is shutdown. $T_{\min}^{GT}$ is the lower limit of the time span of start and stop for GT.

3. Distributionally robust optimization theory

According to Eq. (21), the optimization scheduling model is a function of the prediction error of renewable energy. Due to the limited sample data of renewable energy prediction error, the real distribution of renewable energy prediction error cannot be directly ascertained. Therefore, this paper does not directly obtain the real distribution. But instead, an empirical distribution is established to be used as an estimate of the real distribution, and empirical distribution is founded on past data records of renewable energy prediction error. Due to the limitations of past data records, this section uses the Wasserstein distance to construct a fuzzy set of uncertainty parameter prediction errors. The fuzzy set can be regarded as a sphere with a radius of a, where real distribution mainly distributed around the empirical distribution. The sphere contains all possible real distribution of renewable energy prediction error. The probability distribution of renewable energy historical data mostly fluctuates around the real distribution. The probability distribution fuzzy set of Wasserstein distance focuses more on describing the difference between the real distribution and the empirical distribution. The Wasserstein distance-based fuzzy set independent of prior knowledge is data-driven, and can ensure that the unknown distribution converges to the true distribution. Therefore, it has strong adaptability to the problem studied in this paper, and can make the distributionally robust optimization (DRO) model has good operation ability, and can be less conservative.

3.1. Distributionally robust optimization model

A scheduling method for port energy system in this paper is built based on DRO. The Wasserstein distance-based fuzzy set independent of prior knowledge is data-driven, and can ensure that the unknown distribution converges to the true distribution. It has strong adaptability to the problem studied in this paper, and can make the DRO model has good operation ability, and can be less conservative. Referring to the common two-stage DRO model [31], the two-stage scheduling of port energy system based on DRO can be divided into pre-scheduling in the day-ahead stage and rescheduling in the intraday stage, as shown in Eq. (21). Therefore, a two-stage optimization approach can be suitable for the problem at hand, and would not adversely affect other aspects of the model.

$$\min_{x \in X} \boldsymbol{c}^T\boldsymbol{x} + \sup_{D \in \mathscr{\ell}} E_D(Q(\boldsymbol{x}, \boldsymbol{\omega}^u)), \quad \boldsymbol{A}\boldsymbol{x} \le \boldsymbol{b} \tag{21}$$

In formula, $\mathbf{c}^{\mathrm{T}}$ is the coefficient vector of the pre-scheduling decision variable x. X is the set of pre-scheduling decision variables x. sup $(\cdot)$ is the supremum function. D is true distribution of prediction errors. $\mathscr{\ell}$ is a fuzzy set. $\boldsymbol{\omega}^u$ is an uncertain parameter, which is the prediction error of renewable energy power generation in this paper. $Q(\boldsymbol{x}, \boldsymbol{\omega}^u)$ is the rescheduling cost incurred due to $\boldsymbol{\omega}^u$. $\mathbf{A}$ is the coefficient matrix of the constraint conditions in the pre-scheduling stage. $\mathbf{b}$ is the parameter vector of the constraint conditions in the pre-scheduling stage; $E_D(\cdot)$ indicates mathematics expectation.

Eq. (21) is to minimize the sum of the pre-scheduling cost $\mathbf{c}^{\mathrm{T}}\mathbf{x}$ in the day-ahead stage and the expectation of rescheduling cost $Q(\boldsymbol{x}, \boldsymbol{\omega}^u)$ in the intraday stage. And then, optimal pre-scheduling decision x in the day ahead stage can be obtained, which balances economy and robustness. The expectation of $Q(\boldsymbol{x}, \boldsymbol{\omega}^u)$ is the expectation of the worst distribution in the fuzzy set $\mathscr{\ell}$, as shown in Eq. (22).

$$Q(\boldsymbol{x},\boldsymbol{\omega}^u)=\min\left(\boldsymbol{d}^T\boldsymbol{y}(\boldsymbol{x},\boldsymbol{\omega}^u)\right),\quad \boldsymbol{Z}\boldsymbol{y}(\boldsymbol{x},\boldsymbol{\omega}^u)\le g(\boldsymbol{\omega}^u) \tag{22}$$

In formula, $\boldsymbol{y}(\boldsymbol{x},\boldsymbol{\omega}^u)$ is the decision variable in the rescheduling stage. $\mathbf{d}^{\mathrm{T}}$ is the coefficient vector corresponding to $\boldsymbol{y}(\boldsymbol{x},\boldsymbol{\omega}^u)$. $\mathbf{Z}$ is the coefficient matrix of the constraint conditions in the rescheduling stage. $g(\boldsymbol{\omega}^u)$ is the parameter vector related to $\boldsymbol{\omega}^u$ in the constraint conditions of the rescheduling stage.

From Eq. (21), it can be seen that the min function can be regarded as a pre-scheduling problem in the day-ahead stage. Based on Eqs.(21) and (22), it can be seen that the sup(·) function can be regarded as a rescheduling problem in the intraday stage, following the max-min criterion to improve the worst case scenario in the optimization objective. The day-ahead stage provides the pre-scheduling decision $\mathbf{x}$ for the rescheduling of intraday stage. The intraday stage provides the optimal rescheduling cost $\mathbf{d}^{\mathrm{T}}\mathbf{y}$ under different pre-scheduling decisions for the day-ahead stage. The optimization processes of the day-ahead scheduling and the intraday scheduling are coupled and nested with each other.

3.2. Uncertainty modeling of renewable energy based on wasserstein distance

According to stochastic optimization theory, the uncertainty of renewable energy power generation follows an empirical distribution extracted from historical prediction error data. Based on stochastic optimization theory and combined with robust optimization theory, a fuzzy set is established to obtain the uncertainty set of real distribution, which contains the worst case scenario of real distribution.

Firstly, the empirical distribution $\mathrm{D_e}$ can be determined based on the prediction error sample set $\{\omega_1^{ti},\omega_2^{ti},\cdots,\omega_M^{ti}\}$ of M uncertain variables, and $\mathrm{D_e}$ is used as an estimate of the true distribution D of the prediction error. Following [32,33], $\mathrm{D_e}$ can be constructed, as shown in Eq. (23).

$$D_e=\sum\nolimits_{m=1}^{M}\delta_{\omega_m^{ti}}/M \tag{23}$$

In formula, M represents the sample quantity. $\delta_{\omega_m^{ti}}$ represents the random variable formed by prediction error of renewable energy. The cumulative distribution function can be obtained by assigning 1/M of probability mass to M prediction error of renewable energy, namely empirical distribution. Each prediction error data is a support point for the random variable. Therefore, the empirical distribution is a discrete uniform distribution established on M historical data points, which are independent and identically distributed.

Secondly, a fuzzy set should be constructed based on $\mathrm{D_e}$, which must contain D as much as possible and satisfies $\lim_{M\to\infty} D_e = D$. Furtherly, the Wasserstein distance is used to measure the distance between $\mathrm{D_e}$ and D, and construct a fuzzy set [34]. The definition of Wasserstein distance is shown in Eq. (24).

$$W(D_e,D)=\inf\left\{\int d\left(\boldsymbol{\omega}_e^u,\boldsymbol{\omega}^{ti}\right)\Pi\left(d\boldsymbol{\omega}_e^u,d\boldsymbol{\omega}^{ti}\right)\right\} \tag{24}$$

$$d\left(\boldsymbol{\omega}_e^u,\boldsymbol{\omega}^{ti}\right)=\left\|\boldsymbol{\omega}_e^u-\boldsymbol{\omega}^{ti}\right\| \tag{25}$$

In formula, inf(·) is the infimum function. $\boldsymbol{\omega}_e^u$ and $\boldsymbol{\omega}^{ti}$ are uncertain parameters, which follow the distributions of $\mathrm{D_e}$ and D, respectively. Π(·) is the joint distribution of $\mathrm{D_e}$ and D.

Thirdly, the definition of fuzzy set $\mathscr{O}$ is shown in Eq. (26).

$$\mathscr{O}=\{D\in L(\Xi)|W(D_e,D)<\varepsilon(M)\} \tag{26}$$

In formula, L(Ξ) is all probability distributions in support set Ξ. $\mathscr{O}$ is a Wasserstein sphere, the center of the sphere is $\mathrm{D_e}$, with a radius of $\varepsilon(M)$. In the fixed confidence degree, $\mathscr{O}$ includes all possible probability distributions.

The conservatism of the DRO model can be controlled by $\varepsilon(M)$, which can be calculated by Eq. (27).

$$\varepsilon(M)=F_M\sqrt{-2\ln(1-\alpha)/M},\quad \lim_{M\to\infty}\varepsilon(M)=0 \tag{27}$$

$$F_M=\min\left(\sqrt{2\left[1-\ln M\sum\nolimits_{m=1}^{M}\exp\left(\delta\left\|\omega_m^u-\mu^{ti}\right\|\right)\right]/\delta}\right),\delta>0 \tag{28}$$

In formula, α represents the confidence level. $\mathrm{F_M}$ is a constant. μ^{ti} is the average value of the sample data. δ is a parameter. ω_m^u is the m-th uncertainty parameter.

3.3. Support set based on data driven

The support set Ξ can be calculated by sample data $\{\omega_1^{ti},\omega_2^{ti},\cdots,\omega_M^{ti}\}$ [35]. For the convenience of calculations, the sample set is standardized by the regularization method, as shown in Eq. (29).

$$\theta_m^u = \left(\Gamma^{ti}\right)^{-0.5}\left(\omega_m^{ti} - \mu^{ti}\right), \quad \forall m = 1, 2, \cdots, M \tag{29}$$

In formula, Γ^{ti} is the variance of the sample data. ω_m^{ti} is the m-th sample data.

After normalized, the mean of uncertain parameter sample θ^u is 0, and the variance is I. Assuming Φ is the support set of θ^u, the definition is shown in Eq. (30).

$$\Phi = \left\{\theta^u \in R^T | -l \le \theta_m^u \le l\right\} \quad \forall m = 1, 2, \cdots, M \tag{30}$$

In formula, θ_m^u is the m-th element of θ^u. l is the boundary of θ_m^u.

A reasonable l can be obtained by solving Eq. (31). It not only ensures random event $\theta_m^u \in \Phi$ occurs with a high probability, but also enables Φ small enough to ensure low conservatism.

$$\min_{0 \le l \le l_{\max}} l \quad s.t. \quad \sup_{p^{std} \in \mathscr{P}^{std}} p^{std}(\theta^u \notin \Phi) \le 1 - \varphi \tag{31}$$

In formula, l_{max} is the maximum of l. p^{std} and $\mathscr{P}^{std}$ are probability distribution and fuzzy set of uncertain parameter θ^u, respectively. φ is confidence.

When the optimal l is obtained, a support set based on data driven Ξ can be get by Eq. (32).

$$\Xi = \left(\Gamma^{ti}\right)^{0.5}\Phi + \mu^{ti} \tag{32}$$

4. Modeling and calculation method of Port energy system scheduling based on DRO

In the two-stage optimization of this article, it is necessary to ensure the consumption of renewable energy and the reliable supply for load in the day-ahead stage [36]. The pre-scheduling stage is based on the prediction information of day-ahead stage, and ignores the uncertainty risk caused by prediction errors. In the process of system actual operation, due to the uncertainty of renewable energy, the scheduling strategy obtained in the pre-scheduling stage may not actually be the optimal result. According to the scheduling strategy of pre-scheduling stage, the system will need a lot of power exchange with municipal power grid in the intraday stage, in order to balance supply and demand imbalance caused by renewable energy uncertainty. It results in higher total scheduling cost. Therefore, the rescheduling of system in the intraday stage is needed to stabilize the power fluctuation of renewable energy, when there is a prediction error $\boldsymbol{\omega}^u$ in the renewable energy power generation. The rescheduling is carried out based on the real-time running data and pre-scheduling strategy. During the process of rescheduling, the electricity quantities purchased and sold by power grid and outputs of equipment have been adjusted, the power curtailment of renewable energy power generation and load shedding also have been carried out. Through adjusting pre-scheduling strategy, the rescheduling of intraday stage can optimize the total cost of the above state two stages, which has been applied in Tianjin Port. It also indicates that the two-stage optimization model could effectively address this interdependence between the both stage, which can contribute to the objective of total cost optimization. The distinctions in data characteristics between the day-ahead and intraday stages is shown in Table 1.

Table 1
Distinctions in data characteristics between the day-ahead and intraday stages.

Parameters	Day-ahead stage	Intraday stage
Energy purchase and sale cost	C_t^{main} in Eq. 34	$\widetilde{C}_t^{main}$ in Eq. 38
Carbon emission cost	C_t^{CO2} in Eq. 35	$\widetilde{C}_t^{CO2}$ in Eq. 39
Ammonia production volume	Initial value $Q_t^{NH_3}$	Adjustment value $\widetilde{Q}_t^{NH_3}$
Electricity sold from port to power grid	Initial value P_t^{sell}	Adjustment value $\widetilde{P}_t^{sell}$
Electricity purchased by port from power grid	Initial value P_t^{buy}	Adjustment value $\widetilde{P}_t^{buy}$
Gas consumption of gas turbine	Initial value G_t^{GT}	Adjustment value $\widetilde{G}_t^{GT}$
Gas consumption of gas fired boiler	Initial value G_t^{GB}	Adjustment value $\widetilde{G}_t^{GB}$
Fluctuation penalty cost	C_t^{vary} in Eq. 36	–
Power fluctuation penalty coefficient	c^{vary}	–
Power fluctuation of renewable energy	P_t^{vary}	–
Penalty cost	–	$\widetilde{C}_t^{cut}$ in Eq. 40
Power curtailment penalty coefficient	–	$c^{pr,re}$
Load shedding penalty coefficient	–	$c^{pr,load}$
Power curtailment of wind turbine and PV	–	$P_t^{cut,wt}$ and $P_t^{cut,pv}$
Amount of load shedding	–	$P_t^{cut,load}$

4.1. Objective function

4.1.1. Pre-scheduling cost in the day-ahead stage

The pre-scheduling cost includes such energy purchase and sale cost C_t^{main}, carbon emission cost C_t^{CO2}, and fluctuation penalty cost C_t^{vary} of municipal power grid power, as shown in Eq. (33). The port energy system is connected to the power grid by tie-line through grid-connected inverters and distribution transformers. The fluctuation of tie-line is directly related to the renewable energy power generation. Due to the influence of environmental factors, the renewable energy power generation has fluctuation and uncertainty. The stability of the port energy system under high renewable energy penetration level is more serious, and the power fluctuation of tie-line intensifies, which is not conducive to the safe and stable operation of the power grid. Therefore, North China Power Grid Company introduces fluctuation penalty cost in trading settlement, which can help to guide port to reduce power fluctuation of renewable energy power generation, in order to smooth the tie-line power and maintain safe and stable operation of the power grid.

$$\boldsymbol{c}^T\boldsymbol{x} = \sum\nolimits_{t=1}^{24}\left(C_t^{main} + C_t^{CO2} + C_t^{vary}\right) \tag{33}$$

$$C_t^{main} = -c^{pr,NH_3}Q_t^{NH_3} - c_t^{pr,e,s}P_t^{sell} + c_t^{pr,e,b}P_t^{buy} + c_t^{pr,g}\left(G_t^{GT} + G_t^{GB}\right) \tag{34}$$

$$C_t^{CO2} = c^{pr,CO2}\left[\delta^{g,CO2}\left(G_t^{GT} + G_t^{GB}\right) + \delta^{p,CO2}P_t^{buy}\right] \tag{35}$$

$$\mathrm{C_t^{vary}} = \mathrm{c^{vary}P_t^{vary}}, \mathrm{-P_t^{vary}} \le \left(\mathrm{P_t^{buy}\text{-}P_t^{sell}}\right)\text{-}\left(\mathrm{P_{t-1}^{buy}\text{-}P_{t-1}^{sell}}\right) \le \mathrm{P_t^{vary}} \tag{36}$$

In formula, c^{pr,NH_3} is the sale price of ammonia. $c_t^{pr,e,s}$ and P_t^{sell} are the price and quantity that port sells electricity to municipal power grid. $c_t^{pr,e,b}$ and P_t^{buy} are the price and quantity that port purchases electricity from municipal power grid. $c_t^{pr,g}$ is the price of nature gas. $c^{pr,CO2}$ is the carbon price. $\delta^{g,CO2}$ and $\delta^{p,CO2}$ are respectively the carbon emissions factors of nature gas and municipal power grid. c^{vary} is power fluctuation penalty coefficient of municipal power grid. P_t^{vary} is the power fluctuation of municipal power grid caused by renewable energy.

4.1.2. Rescheduling cost in the intraday stage

Due to the unknown true distribution of $\boldsymbol{\omega}^u$, within the Wasserstein distance-based fuzzy set $\mathscr{D}$, the goal of Eq. (36) is to minimize the rescheduling cost under the worst-case scenario. The rescheduling cost includes such energy purchase and sale cost $\widetilde{C}_t^{main}$, carbon emission cost $\widetilde{C}_t^{CO2}$, and penalty cost $\widetilde{C}_t^{cut}$ for power curtailment of renewable energy power generation and load shedding, as shown in Eq. (37).

$$\sup_{D\in\mathscr{D}} E_D(Q(\boldsymbol{x},\boldsymbol{\omega}^u)) = \sup_{D\in\mathscr{D}} E_D\left(min\sum\nolimits_{t=1}^{T}\left(\widetilde{C}_t^{main} + \widetilde{C}_t^{CO2} + \widetilde{C}_t^{cut}\right)\right) \tag{37}$$

$$\widetilde{C}_t^{main} = -c^{pr,NH_3}\widetilde{Q}_t^{NH_3} - c_t^{pr,e,s}\widetilde{P}_t^{sell} + c_t^{pr,e,b}\widetilde{P}_t^{buy} + c_t^{pr,g}\left(\widetilde{G}_t^{GT} + \widetilde{G}_t^{GB}\right) \tag{38}$$

$$\widetilde{C}_t^{CO2} = c^{pr,CO2}\left[\delta^{g,CO2}\left(\widetilde{G}_t^{GT} + \widetilde{G}_t^{GB}\right) + \delta^{p,CO2}\widetilde{P}_t^{buy}\right] \tag{39}$$

$$\widetilde{C}_t^{cut} = c^{pr,re}\left(P_t^{cut,wt} + P_t^{cut,pv}\right) + c^{pr,load}P_t^{cut,load} \tag{40}$$

In formula, $\widetilde{Q}_t^{NH_3}$ is the adjustment value of ammonia production volume at time t. $\widetilde{P}_t^{sell}$ and $\widetilde{P}_t^{buy}$ are the adjustment value of the quantity that port sells electricity to municipal power grid, and port purchases electricity from municipal power grid. $c_t^{pr,g}$ is the price of nature gas. $\widetilde{G}_t^{GT}$ and $\widetilde{G}_t^{GB}$ are the adjustment values for gas consumption of gas turbine and gas fired boiler, respectively. $c^{pr,re}$ and $c^{pr,load}$ are penalty coefficients for the power curtailment of renewable energy power generation and load shedding. $P_t^{cut,wt}$ $P_t^{cut,pv}$ and $P_t^{cut,load}$ are the quantity for the power curtailment of wind turbine, photovoltaic and load shedding.

4.2. Constraints

4.2.1. Day-ahead stage

The pre-scheduling in the day-ahead stage needs to meet various equipment constraints, as shown in Section 2. In addition, it is also necessary to meet municipal power grid operation constraints and energy balance constraints.

(1) Municipal power grid operation constraints

$$0 \le P_t^{buy} \le U_t^{MPG}P_{\max}^{MPG} \tag{41}$$

$$0 \le P_t^{sell} \le \left(1 - U_t^{MPG}\right)P_{\max}^{MPG} \tag{42}$$

In formula, U_t^{MPG} is 0–1 variable. $U_t^{MPG}=1$ represents port purchases electricity from the municipal power grid. $U_t^{MPG}=0$ represents port sells electricity to the municipal power grid. $P_{\max}^{MPG}$ is the upper limit of exchange power between port and municipal power grid.

(2) Energy balance constraints

$$P_t^{buy}+P_t^{GT}+P_t^{WT}+P_t^{PV}=P_t^{sell}+P_t^{EC}+P_t^{P2H}+P_t^{H_2,C}+P_t^{AS}+P_t^{NH_3}+P_t^{load,e} \tag{43}$$

$$H_t^{GT}+H_t^{GB}+H_t^{HES,dis}=H_t^{HES,ch}+H_t^{AC}+H_t^{load,h} \tag{44}$$

$$L_t^{EC}+L_t^{AC}=L_t^{load,c} \tag{45}$$

In formula, P_t^{WT} and P_t^{PV} respectively represent the power of wind turbine and photovoltaic. $P_t^{load,e}$, $H_t^{load,h}$ and $L_t^{load,c}$ are electric load, heating load, and cooling load at time t.

4.2.2. Intraday stage

On the basis of pre-scheduling, the port energy system should be adjusted through rescheduling of intraday stage. The rescheduling in the intraday stage should also meet the equipment operation constraints in Section 2. In addition, it is also necessary to meet the curtailment constraints of renewable energy and load, and energy balance constraints.

(1) Curtailment constraints of renewable energy and load

$$0\le P_t^{cut,i}\le P_t^{i}+\omega^u,\quad i=\{WT,PV\} \tag{46}$$

$$0\le P_t^{cut,load}\le P_t^{load,e} \tag{47}$$

In the formula, $P_t^{cut,i}$ and $P_t^{cut,load}$ respectively represent the reduction of renewable energy power generation and load. ω^u is the prediction error of renewable energy power generation.

(2) Energy balance constraints

$$\widetilde{L}_t^{EC}+\widetilde{L}_t^{AC}=0 \tag{48}$$

$$\widetilde{H}_t^{GT}+\widetilde{H}_t^{GB}+\widetilde{H}_t^{HES,dis}=\widetilde{H}_t^{HES,ch}+\widetilde{H}_t^{AC} \tag{49}$$

$$\widetilde{P}_t^{buy}+\widetilde{P}_t^{GT}+P_t^{cut,load}+\omega^u=\widetilde{P}_t^{sell}+\widetilde{P}_t^{EC}+\widetilde{P}_t^{P2H}+\widetilde{P}_t^{H_2,C}+\widetilde{P}_t^{AS}+\widetilde{P}_t^{NH_3}+P_t^{cut,WT}+P_t^{cut,PV} \tag{50}$$

4.3. Reconstruction of scheduling model for port energy system

The two-stage scheduling model of port energy system based on DRO can be expressed as a min-max-min three-layer optimization as shown in Eq. (51).

$$\min_{x\in X}\boldsymbol{c}^T\boldsymbol{x}+\sup_{D\in\mathscr{\ell}}E_D\left(\min\left(\boldsymbol{d}^T\boldsymbol{y}(\boldsymbol{x},\boldsymbol{\omega}^u)\right)\right) \tag{51}$$

Because Eq. (50) contains D, $D\in\mathscr{\ell}$ and $\boldsymbol{\omega}^u\in\Xi$, the constraint contains prediction error random variables and becomes an infinite limit. Therefore, the two-stage scheduling model based on DRO belongs to a semi-infinite programming model, which is difficult to directly solve. Therefore, this section reconstructs it into the mixed integer linear programming model for solution through strong duality theorem, and the reconstruction process is as follows.

Firstly, according to strong duality theorem, the worst-case scenario expectation can be rewritten as Eq. (52).

$$\sup_{D\in\mathscr{\ell}}E_D(Q(\boldsymbol{x},\boldsymbol{\omega}^u))=\inf_{\sigma\ge0}\left\{\sum\nolimits_{m=1}^{M}\sup_{\omega^u\in\Xi}\left(Q(\boldsymbol{x},\boldsymbol{\omega}^u)-\sigma\left\|\boldsymbol{\omega}^u-\boldsymbol{\omega}_m^{ti}\right\|\right)/M+\sigma\varepsilon\right\} \tag{52}$$

In formula, σ is a dual variable.

Secondly, Eq. (51) under support set Ξ can be equivalently represented as Eq. (53).

$$\min_{x\in X,\sigma\ge0}\boldsymbol{c}^T\boldsymbol{x}+\sum\nolimits_{m=1}^{M}\sup_{\omega^u\in\Xi}\left(Q(\boldsymbol{x},\boldsymbol{\omega}^u)-\sigma\left\|\boldsymbol{\omega}^u-\boldsymbol{\omega}_m^{ti}\right\|\right)/M+\sigma\varepsilon \tag{53}$$

$$s.t.\quad \boldsymbol{A}\boldsymbol{x}\le\boldsymbol{b},\quad \boldsymbol{Z}\boldsymbol{y}(\boldsymbol{x},\boldsymbol{\omega}^u)\le g(\boldsymbol{\omega}^u),\quad \forall\boldsymbol{\omega}^u\in\Xi \tag{54}$$

In formula, $\boldsymbol{A}\boldsymbol{x}\le\boldsymbol{b}$ represents the constraints of pre-scheduling stage. $\boldsymbol{Z}\boldsymbol{y}(\boldsymbol{x},\boldsymbol{\omega}^u)\le g(\boldsymbol{\omega}^u)$ represents the constraints of rescheduling

stage.

Thirdly, Eq. (53) also contains a max-min problem, which is difficult to solve directly. Therefore, auxiliary variable β_m needs to be introduced, and Eq. (53) is rewrote to Eq. (55).

$$\min_{x\in X,\sigma\geq 0} \boldsymbol{c}^T\boldsymbol{x} + \sum\nolimits_{m=1}^{M} \beta_m/M + \sigma\varepsilon \tag{55}$$

$$s.t.\begin{cases} \sup\limits_{\omega^u\in\Xi}\left(Q(\boldsymbol{x},\boldsymbol{\omega}^u) - \sigma\left\|\boldsymbol{\omega}^u - \boldsymbol{\omega}_m^{ti}\right\|\right) \leq \beta_m, \quad \forall m = 1,2,\cdots,M \\ \boldsymbol{A}\boldsymbol{x} \leq \boldsymbol{b}, \quad \boldsymbol{Z}\boldsymbol{y}(\boldsymbol{x},\boldsymbol{\omega}^u) \leq g(\boldsymbol{\omega}^u), \quad \forall\boldsymbol{\omega}^u \in \Xi \end{cases} \tag{56}$$

If $Q(\boldsymbol{x},\boldsymbol{\omega}^u)$ is a convex function about variable $\boldsymbol{\omega}^u$ [37], then the optimal solution of $\sup\limits_{\omega^u\in\Xi}(Q(\boldsymbol{x},\boldsymbol{\omega}^u) - \sigma\left\|\boldsymbol{\omega}^u - \boldsymbol{\omega}_m^{ti}\right\|)$ must be obtained on the upper and lower bounds $(\boldsymbol{\omega}^s,\boldsymbol{\omega}_x)$ of $\boldsymbol{\omega}^u$ or $\widehat{\boldsymbol{\omega}}_n \in \Xi, \quad \forall m = 1,2,\cdots,M$. Obviously, $Q(\boldsymbol{x},\boldsymbol{\omega}^u)$ is a linear function of $\boldsymbol{\omega}^u$. In addition, $\boldsymbol{y}(\boldsymbol{x},\boldsymbol{\omega}^u)$ and $g(\boldsymbol{\omega}^u)$ also have a linear relationship with $\boldsymbol{\omega}^u$. Therefore, under the support set Ξ, $\sup\limits_{\omega^u\in\Xi}(\boldsymbol{y}(\boldsymbol{x},\boldsymbol{\omega}^u) - g(\boldsymbol{\omega}^u))$ takes value within the upper and lower bounds of $\boldsymbol{\omega}^u$.

In conclusion, the scheduling model of port energy system based on DRO can be reconstructed into a mixed integer linear programming model, which is easy to solve, such as in Eqs.(57) and (58). The error variable $\boldsymbol{\omega}^u$ of renewable energy power generation is no longer included in Eqs.(57) and (58). Therefore, this model has become a mixed integer linear programming problem, which can be solved directly through commercial solvers.

$$\min_{x\in X,\sigma\geq 0} \boldsymbol{c}^T\boldsymbol{x} + \sum\nolimits_{m=1}^{M} \beta_m/M + \sigma\varepsilon \tag{57}$$

$$s.t.\begin{cases} Q(\boldsymbol{x},\boldsymbol{\omega}^s) - \sigma\left\|\boldsymbol{\omega}^s - \boldsymbol{\omega}_m^{ti}\right\| = \boldsymbol{d}^T\boldsymbol{y}(\boldsymbol{x},\boldsymbol{\omega}^s) - \sigma 1^T\left(\boldsymbol{\omega}^s - \boldsymbol{\omega}_m^{ti}\right) \leq \beta_m \\ Q(\boldsymbol{x},\boldsymbol{\omega}_x) - \sigma\left\|\boldsymbol{\omega}_x - \boldsymbol{\omega}_m^{ti}\right\| = \boldsymbol{d}^T\boldsymbol{y}(\boldsymbol{x},\boldsymbol{\omega}_x) - \sigma 1^T\left(\boldsymbol{\omega}_x - \boldsymbol{\omega}_m^{ti}\right) \leq \beta_m \\ Q\left(\boldsymbol{x},\boldsymbol{\omega}_m^{ti}\right) - \sigma\left\|\boldsymbol{\omega}_m^{ti} - \boldsymbol{\omega}_m^{ti}\right\| = \boldsymbol{d}^T\boldsymbol{y}\left(\boldsymbol{x},\boldsymbol{\omega}_m^{ti}\right) \leq \beta_m, \quad \forall m = 1,2,\cdots,M \\ \boldsymbol{A}\boldsymbol{x} \leq \boldsymbol{b}, \quad \sigma \geq 0, \quad \boldsymbol{Z}\boldsymbol{y}(\boldsymbol{x},\boldsymbol{\omega}^s) \leq g(\boldsymbol{\omega}^s), \quad \boldsymbol{Z}\boldsymbol{y}(\boldsymbol{x},\boldsymbol{\omega}_x) \leq g(\boldsymbol{\omega}_x) \end{cases} \tag{58}$$

Significantly, the rescheduling decision is transformed to a prediction error function in Eqs.(57) and (58), the final result of two-stage scheduling based on DRO is the pre-scheduling result.

5. Example analysis

By building rooftop photovoltaic (PV) and offshore wind turbine (WT), Tianjin Port builds a integrate energy system wherein renewable energy constitutes the main body of energy, supplemented by natural gas distributed energy system, and coordinated with municipal power grid (MPD), in order to optimize the synthetical efficiency for low-carbon energy utilization.

The research results of this article have been demonstrated in the northern port of Tianjin Port. From the short-running operational effect, hydrogen energy is treated as a green energy carrier in Tianjin Port that can enhance the capacity of renewable energy utilization and promote the low-carbon transition of port energy system. Moreover, the economy and flexibility of energy system in Tianjin Port can be improved by the ammonia synthesis after hydrogen production using renewable energy.

Therefore, Simulation was conducted in Part V using real data from Tianjin Port. Part V can obtain various load and device information required for simulation through actual data from Tianjin Port. The load in the northern port mainly comes from the ship shore power and the heating and cooling requirements of container terminal. A notice will be issued before the ship arrives at the northern port, the port load can be calculated according to the notice, and the level of uncertainty is small. Therefore, this article has not yet considered the uncertainty of load. With the development of demonstration areas, the uncertainty of port load will be considered in the future. The results of example analysis were consistent with the Tianjin Port trial running data. It can demonstrate that the scheduling method based on distributionally robust optimization has outstanding advantages in the computing time and renewable energy utilization to improve the flexibility and economy of energy system in Tianjin Port. Example analysis verified this article from three sections.

Section 5.2 analyzes the impact of load rate adjustment on the safety constraints of the ammonia synthesis section, confirms the rationality of Eqs. (4) and (5) to describe the control inertia of the ammonia synthesis reaction in this article. From comparison of P2H2A system under various optimization methods, the advantage of DRO in the renewable energy utilization and the regulation ability of hydrogen storage tank is confirmed.

Section 5.3 shows comparison results of deterministic optimization, stochastic optimization, robust optimization, and confirms that DRO can improve the capacity of anti-risk for stochastic optimization and overcome the conservatism of robust optimization on the one hand, and consider economy and robustness on the other hand. The pre-scheduling results based on DRO are consistent with the Tianjin Port operation data.

Section 5.4 illustrates that DRO can reflect the decision-making risk preference of the port energy system by adjusting the Wasserstein distance-based sphere radius, and confirms that DRO considers the uncertainty of probability distribution and has the

advantages of stochastic optimization and robust optimization.

5.1. Example settings

The energy purchase and sale prices at Tianjin Port are shown in Fig. 3. Equipment parameters of Tianjin Port are shown in Table 2. Referring to the market price in recent years, the sale price of ammonia at the port is set to 393.96 $/ton. The port has one offshore wind-farm and one rooftop photovoltaic. The predicted error data of renewable energy power generation is sourced from the publicly available data of Tennet [38]. The scheduling period is 24 h, and the time interval of scheduling is set to 1 h. In the example analysis, this paper uses the YALMIP tool kit in MATLAB to call CPLEX to solve the scheduling model of port energy system based on DRO. The computer parameters are Intel Corei5 1.99 GHz CPU and 8 GB memory.

5.2. Simulation verification of scheduling constrains for ammonia synthesis

To verify the impact of load rate adjustment on the safety constraints of the ammonia synthesis section, the model of ammonia synthesis section was established in this paper, such as the ammonia converter, circulation recovery, and ammonia separation. The simulation results of ammonia production volume, hydrogen production volume, ammonia converter pressure and temperature are shown in Fig. 4. The load rate adjustment command of ammonia synthesis section is shown in Fig. 4 (a) by the blue solid line and green solid line, which decreases from 0.6 ton/h to 0.2 ton/h after 0.4 h or 1 h. The response processes are shown by the orange solid line (0.4 h) and yellow solid line (1 h) in Fig. 4, according to the load rate adjustment command of ammonia synthesis section. Security constrain is shown by the black solid line in Fig. 4 (c) and Fig. 4 (d).

The impact of ramp rate of load rate adjustment on the safety constraints of ammonia synthesis section is analyzed as follows. When the ramp rate of load rate adjustment is relatively small, it can ensure that the ammonia synthesis reaction transitions smoothly to the new steady state, and the temperature and pressure of the ammonia converter meet safety constraints. When the ramp rate of load rate adjustment is relatively large, due to the large inertia of mass and heat transfer in the ammonia synthesis section, it is difficult to adjust in a timely manner. It results in the significant fluctuation of temperature and pressure of ammonia converter, which violates safety constraints. Using Eqs. (4) and (5) to describe the control inertia of the ammonia synthesis reaction in this article is more reasonable, and the time interval of scheduling of 1 h is reasonable.

Using the system parameters given in Section 5.1, the running status of P2H2A can be calculated and shown in Fig. 5, based on the distributionally robust optimization scheduling model of port energy system in Section 4.

Fig. 5 shows the curves of hydrogen production volume, residual capacity of hydrogen storage tank and ammonia production volume under different scheduling method, such as deterministic optimization, robust optimization and DRO. As shown in Fig. 5 (a), compared to deterministic optimization, DRO utilizes almost the same amount of renewable energy power generation without causing the power curtailment of wind turbine and photovoltaic. As shown in Fig. 5 (b) and Fig. 5 (c), compared to deterministic optimization, DRO can reduce the smoothness of ammonia production volume slightly, which can make the residual capacity of the hydrogen storage tank no longer touch the upper limit constraint and enhance the robustness of the scheduling method. Compared with robust optimization, DRO better utilizes the renewable energy power generation and the regulation ability of hydrogen storage tank, which can effectively improve economic benefits of P2H2A.

5.3. Scheduling result analysis of distributionally robust optimization

The probability distribution of prediction error of renewable energy power generation at each prediction time scale was obtained by kernel density estimation, as shown in Fig. 6. With the inverse function of prediction error probability distribution, the output interval of renewable energy power generation can be obtained, and the confidence level is 95%. The scenarios of renewable energy power generation can be obtained by K-means clustering. The number of scenarios is 20, and the radius of sphere is 1 MW.

The comparison results of deterministic optimization, stochastic optimization, robust optimization, and DRO are shown in Table 3.

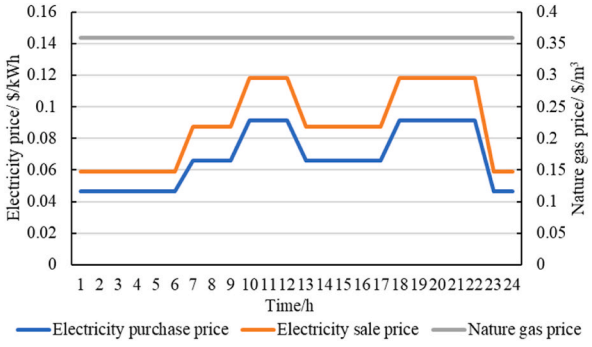

Fig. 3. Energy purchase and sale price of port.

Table 2
Equipment parameters of port.

Equipment	Parameters			
Municipal power grid	Name	Value	Name	Value
	Power limit for purchasing and selling electricity/MW	7/7	Power fluctuation penalty coefficient/$/MW	28.14
	Carbon emission coefficient/ton/MWh	0.6	–	–
Nature gas	Heat value/kWh/m^3	9.87	Carbon emission coefficient/kg/m^3	2.262
Electrolyzer	Upper limit of hydrogen production power/MW	6	Hydrogen production efficiency/%	70
Hydrogen storage tank	Installed capacity/MWh	5	Hydrogen storage/release efficiency/%	98/98
	Starting and ending SOC/%	50/50	Upper limit of hydrogen storage/release power/MW	2/2
	Upper and lower limits of SOC/%	90/10	–	–
Ammonia synthesis	Ammonia production volume/ton/h	0.64	Fixed power consumption/MW	0.055
Gas turbine	Upper and lower limits of electric power/MW	3/0.3	Upper and lower limits of ramp rate/MW	1/−1
	Lower limit of the time span of start and stop/h	3/3	Power generation and heat generation efficiency/%	30/50
Gas fired boiler	Upper limit of thermal power/MW	2.5	Heat generation efficiency/%	90
Heat energy storage device	Installed capacity/MWh	15	Charge/discharge efficiency/%	98/98
	Starting and ending SOC/%	50/50	Upper limit of charge/discharge power/MW	1.3/1.3
	Upper and lower limits of SOC/%	90/10	–	–
Absorption cooler	Upper limit of cooling power/MW	0.8	Cooling efficiency/%	130
Electric cooler	Upper limit of cooling power/MW	0.8	Cooling efficiency/%	400
Others	Cost coefficient of wind power curtailment/$/MW	42.21	Cost coefficient of load shedding/$/MW	351.75
	Cost coefficient of photovoltaic curtailment/$/MW	0.3	Carbon cost coefficient/$/ton	35.18

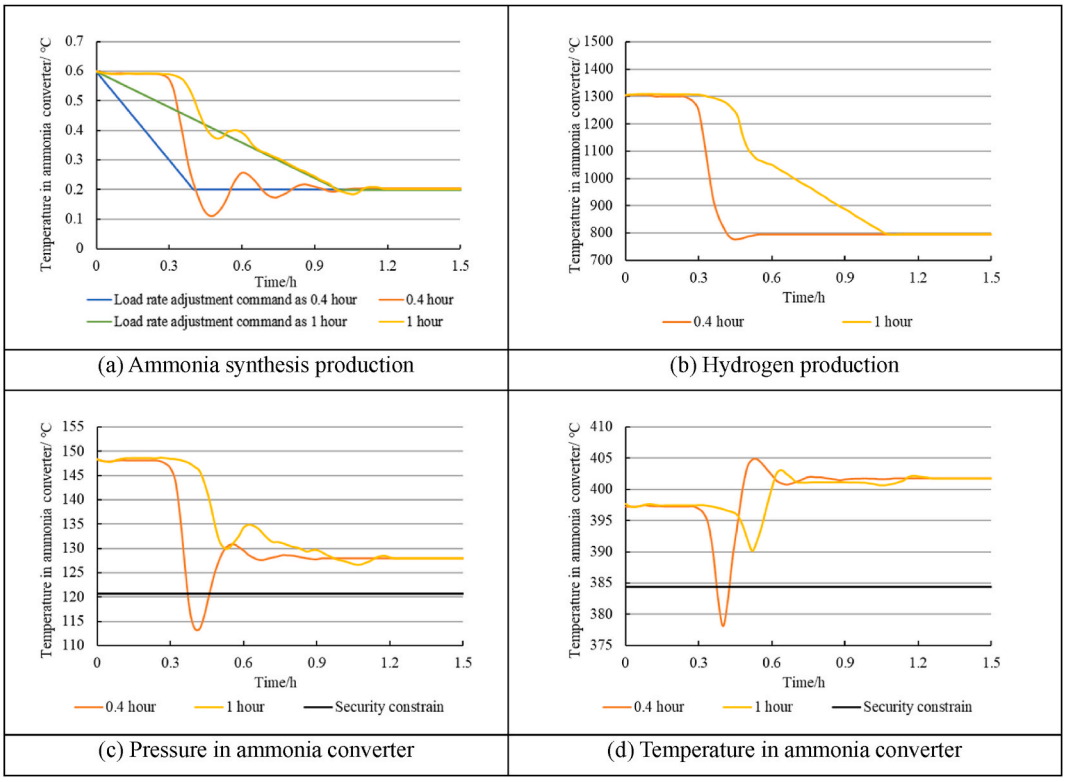

Fig. 4. The dynamic responses of the ammonia synthesis section under different ramp rate of load rate.

Random optimization, robust optimization, and DRO are all two-stage scheduling methods. Deterministic optimization is a single stage scheduling method, which does not need to consider the rescheduling process and has no related cost.

As shown in Table 3, the total scheduling cost of deterministic optimization is the lowest. But this does not mean that deterministic optimization is superior to uncertain optimization. The pre-scheduling of deterministic optimization is based on the prediction information of day-ahead stage, without considering the uncertainty risk and rescheduling cost caused by prediction errors. In the

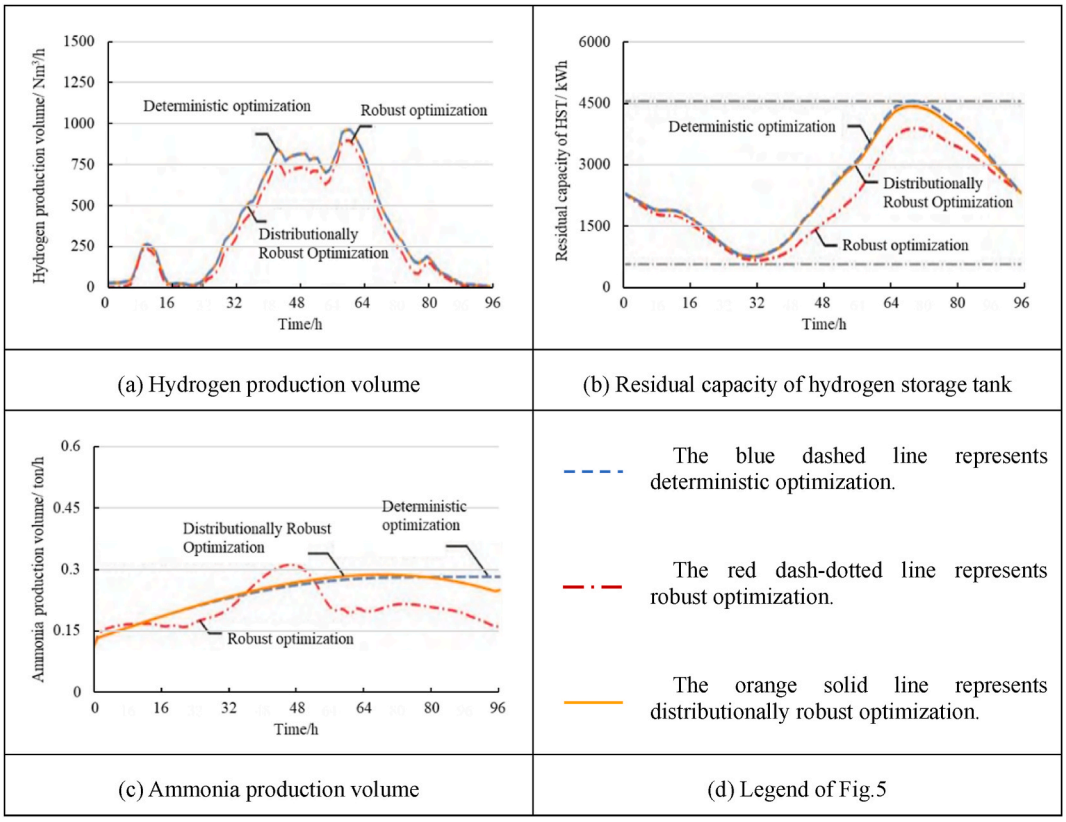

Fig. 5. Result comparison of P2H2A system under various optimization methods.

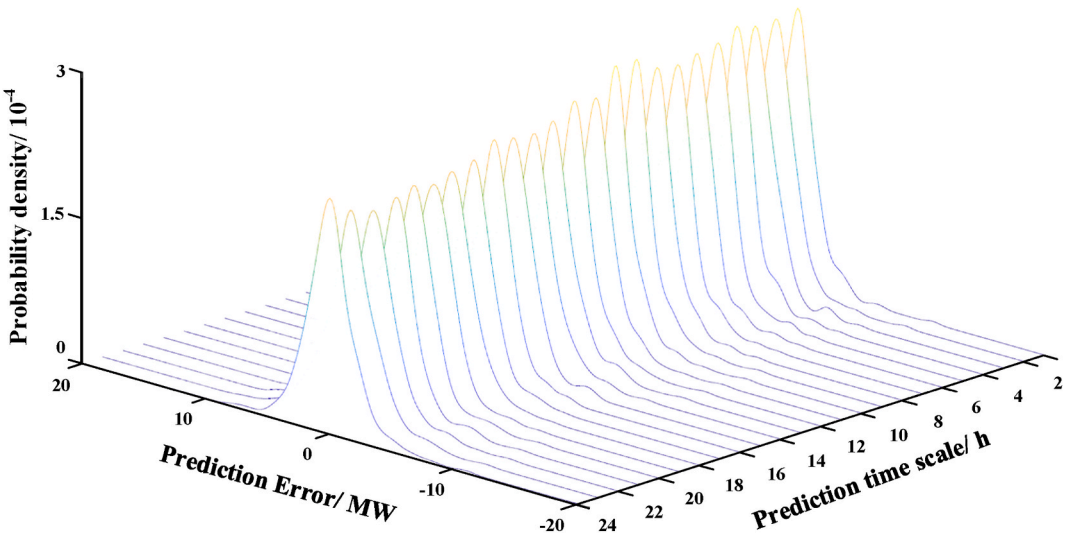

Fig. 6. Forecast error probability distribution.

intraday stage, deterministic optimization requires a large amount of power exchange between port and municipal power grid, in order to solve the power imbalance problem caused by prediction errors of renewable energy power generation. It results in higher actual scheduling costs.

In uncertain optimization methods, stochastic optimization has the lowest pre-scheduling and rescheduling costs, because they are calculated based on precise probability distribution. However, a precise probability distribution will result in an overly optimistic risk expectation in the intraday stage. Insufficient power exchange between port and municipal power grid in the day-ahead stage will

Table 3
Scheduling results under different optimization methods.

Name	Pre-scheduling cost/$	Rescheduling cost/$	Total scheduling cost/$
Deterministic optimization	6756.67	0	6756.67
Stochastic optimization	6757.77	635.81	7393.58
Robust optimization	8429.96	9569.44	17999.4
Distributionally robust optimization	7001.95	2736.01	9737.96

reduce the capability of anti-risk of stochastic optimization in the intraday stage. It results in the worst robustness of stochastic optimization.

Robust optimization has the highest pre-scheduling and rescheduling costs, which are calculated based on the prediction error of worst-case scenario. In the day-ahead stage, robust optimization requires increasing power exchange between port and municipal power grid to enhance the capacity of anti-risk in the intraday stage, and has good robustness. However, it will result in the highest pre-scheduling cost and the worst economic property.

The pre-scheduling and rescheduling costs of DRO are between stochastic optimization and robust optimization. The main reason is that pre-scheduling of DRO is made based on the forecasting error and its probability distribution under worst-case scenario. With the complementary advantages of stochastic optimization and robust optimization, DRO can improve the capacity of anti-risk for stochastic optimization and overcome the conservatism of robust optimization on the one hand, and give consideration to economy and robustness on the other hand.

In this paper, the rescheduling decision is transformed to a prediction error function in Eqs.(57) and (58), so the final result of two-stage scheduling based on DRO is the pre-scheduling result. The composition of pre-scheduling cost under different optimization methods shown in Table 4.

As shown in Table 4, by comparison with deterministic optimization and stochastic optimization, DRO and robust optimization have higher pre-scheduling cost, due to the increase in electricity purchases from the municipal power grid by port. At the same time, both also have higher carbon emission cost. The main reason is that in order to improve the capacity of anti-risk in the intraday stage, the pre-scheduling scheme increased the electricity purchased from the municipal power grid, which is dominated by thermal power plants. The increase in electricity purchase results in lower nature gas purchase cost of robust optimization and DRO. Robust optimization is expected to have highest power fluctuation cost based on the worst-case scenario, and there was no significant difference among the others. The sales revenue of liquid ammonia is 243.66 $ in robust optimization, and that of DRO is 294.91 $. Compared with 243.66 $, a 21.03 per cent rise on the sales revenue of liquid ammonia of DRO.

The detailed results of pre-scheduling based on DRO are shown in Fig. 7.

By comparison with absorption cooler in Table 2, electric cooler has higher cooling efficiency. As shown in Fig. 7 (a) and Fig. 7 (d), the cooling load is mainly supplied by electric cooler, while the rest is supplied by absorption cooler. During the period from 8:00 to 19:00, the renewable energy power generation is less than the electric load. Due to the high electricity purchase price during this period, the cooling load is mainly supplied by absorption cooler, in order to reduce the cost of electricity purchased from the municipal power grid (MPD).

As shown in Fig. 7 (b) and Fig. 7 (d), the renewable energy power generation is less than the electric load, and both the electric and heating loads are mainly supplied by gas turbines, during the period from 8:00 to 19:00. Surplus thermal energy is stored in the heat energy storage device, which can shift the above thermal energy to the period of 21:00–6:00 for use, lowering the cost of thermal energy supply. During the period from 21:00 to 6:00, the renewable energy power generation is relatively high, so the gas turbine will be kept at lowest possible power to provide reserve capacity. The heating load is mainly supplied by the gas boiler.

As shown in Fig. 7 (c) and Fig. 7 (d), hydrogen generation by water electrolysis can improve the capacity of renewable energy utilization, during the periods of 6:00–7:00 and 21:00–5:00. The ammonia synthesis system also tends to operate during this period. During the period from 9:00 to 18:00, the ammonia synthesis system operates stably on a lower power level, in order to reduce the cost of electricity purchased from the municipal power grid. During the period from 21:00 to 6:00, there was no significant power fluctuation between port and municipal power grid. The mainly reason is that ammonia synthesis after hydrogen production by water electrolysis can adapt to the uncertain properties of renewable energy, which can effectively stabilize power fluctuation. As shown in Fig. 7 (d), the power exchange between the port and the municipal power grid is mainly used as a supplementary method, when the port energy system is unable to satisfy the electric load demand or consume renewable energy power generation. Renewable energy

Table 4
Composition of pre-scheduling cost under different optimization methods.

Name	Deterministic optimization	Stochastic optimization	Robust optimization	Distributionally robust optimization
Electricity purchase/$	1185.43	1130.52	4158.11	1694.43
Electricity sale/$	−635.89	−729.30	−739.77	−726.20
Nature gas purchase/$	4932.62	5070.17	3374.94	4771.72
Carbon emission/$	1339.94	1369.26	1616.95	1406.03
Power fluctuation/$	144.01	157.33	263.39	150.88
Liquid ammonia sale/$	−209.44	−240.21	−243.66	−294.91
Pre-scheduling cost/$	6756.67	6757.77	8429.96	7001.95

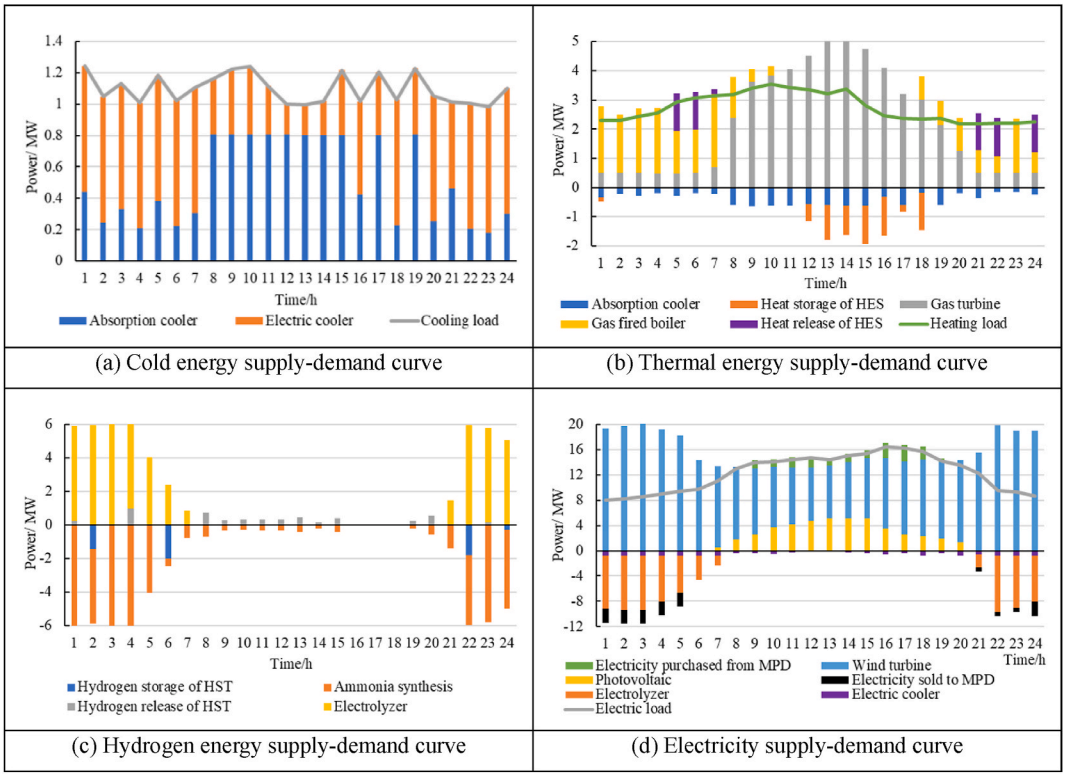

Fig. 7. Results of pre-scheduling based on distributionally robust optimization.

still constitutes the main body of energy at the port area.

5.4. *Sensitivity analysis of distributionally robust optimization scheduling*

Distributionally robust optimization is an uncertain optimization method that combines stochastic optimization and robust optimization. Through the analysis in Part III, the Wasserstein distance-based sphere radius has a clear meaning, the sphere radius of its Wasserstein distance-based fuzzy set determines whether DRO favors risk neutral stochastic optimization or risk averse robust optimization. The sensitivity analysis in Section 5.4 can provide intuitive data as a reference for decision-makers. The original work of this paper is to do the sensitive analysis of α and M. But according to feedback from decision-makers, it is indeed not as intuitive as the sensitivity analysis of Wasserstein distance. Therefore, in order to meet the demand of project, this section conducted a sensitivity analysis of Wasserstein distance-based sphere radius, without addressing the sensitivity analysis of α and M. The relationship between pre-scheduling cost and Wasserstein distance-based sphere radius is shown in Fig. 8, which indicates the impact of Wasserstein distance-based sphere radius on risk preference.

As shown in Fig. 8, the pre-scheduling costs of stochastic optimization and robust optimization are constant, which have nothing to do with Wasserstein distance-based sphere radius. The pre-scheduling cost of DRO falls between stochastic optimization and robust optimization, and varies with the Wasserstein distance-based sphere radius. As the Wasserstein distance-based sphere radius increases, the pre-scheduling cost of DRO gradually deviates from risk neutral stochastic optimization and leans towards risk averse robust optimization.

When leaning towards stochastic optimization, pre-scheduling decision tends to be economic. It indicates that the decision-maker believes that the probability distribution of uncertain variables is accurate enough or historical data is adequate to construct the fuzzy set. When leaning towards robust optimization, pre-scheduling decision tends towards robustness. It indicates that the decision-maker believes that significant risks will arise in the future, and priority should be given to the reliability of the pre-scheduling decision. In summary, DRO can reflect the decision-making risk preference of the port energy system by adjusting the Wasserstein distance-based sphere radius. It can achieve reasonable scheduling that balances economy and robustness.

When the Wasserstein distance-based sphere radius remains constant, distributionally robust optimization scheduling is also affected by the number of scenarios, which is used to build the Wasserstein distance-based fuzzy set. The relationship between pre-scheduling cost (Black dots), calculation time (red line) and number of scenarios is shown in Fig. 9.

As shown in Fig. 9, when the number of scenarios is small, the pre-scheduling cost is divergent and the variance is large. It indicates that a small number of scenarios are difficult to accurately reflect the true distribution of renewable energy power generation, which has significant uncertainty. As the number of scenarios increases, the variance gradually decreases, which can promote the Wasserstein

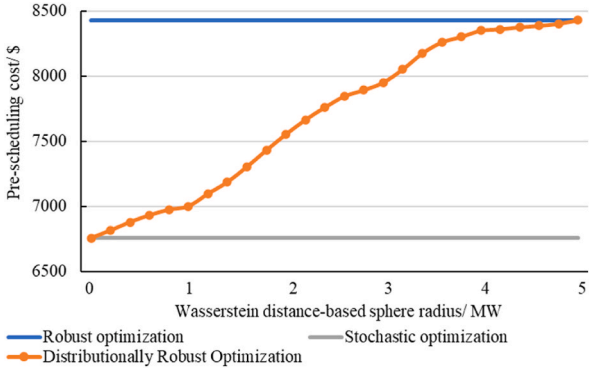

Fig. 8. Pre-scheduling cost under different Wasserstein distance-based sphere radius.

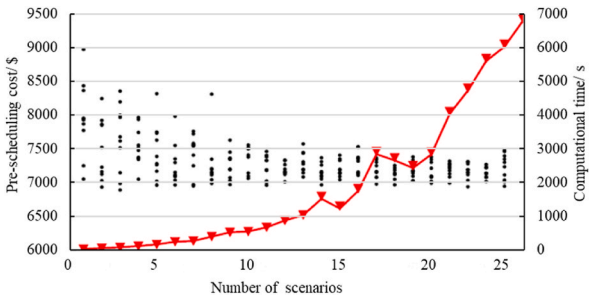

Fig. 9. Pre-scheduling costs and their calculation time under different number of scenarios.

distance-based fuzzy set to converge to the true distribution. However, the calculation time increases sharply with the increase of the number of scenarios. Therefore, it is necessary to analyze the computational efficiency of the scheduling model based on DRO.

Before the model reconstruction, there were 2111 decision variables of pre-scheduling and rescheduling. After the model reconstruction, there were 3071 decision variables of pre-scheduling and linear decision rule. The number of decision variables after model reconstruction significantly increased. However, when the number of scenarios in Fig. 9 is greater than 15, the pre-scheduling cost will no longer fluctuate significantly, and the calculation time is in the range of 1200 s–6600 s. It can meet the demands of day-ahead scheduling calculation time. Therefore, this paper proposed model can meet the demand for computing efficiency.

In addition, DRO considers the uncertainty of probability distribution, and has the advantages of stochastic optimization and robust optimization, which are illustrated by the following example. Assuming that the prediction error of renewable energy power generation corresponds to the normal distribution, five different mean values are selected to generate renewable energy power generation scenarios by Latin hypercube sampling. The pre-scheduling costs under different mean values are shown in Table 5.

As shown in Table 5, the deterministic optimization does not consider prediction errors, resulting in the lowest pre-scheduling cost and overly optimistic risk expectation. Meanwhile, its pre-scheduling cost remains unchanged, and it's impossible to adjust the risk expectation based on historical prediction error data.

Stochastic optimization is based on probability distribution information to conduct optimal scheduling. When the actual value of renewable energy power generation is greater than the predicted value (i.e., the mean value is greater than 0), its pre-scheduling cost approaches the pre-scheduling cost of deterministic optimization, reflecting optimistic risk expectation. When the actual output of renewable energy is less than the predicted output (i.e., the mean value is less than 0), its pre-scheduling cost increases as the mean value decreases, reflecting negative risk expectation. However, it does not consider the uncertainty of probability distribution, so its robustness is poor.

Robust optimization has the highest pre-scheduling cost, indicating its strongest robustness. But it does not utilize probability distribution information, so its economy is the worst. It shows an overly negative attitude towards risk expectation.

Table 5
Pre-scheduling costs under different mean values.

Mean values/MW	−1	−0.5	0	0.5	1
Deterministic optimization/$	6756.67	6756.67	6756.67	6756.67	6756.67
Stochastic optimization/$	7189.95	6897.13	6757.77	6768.08	6814.63
Robust optimization/$	8653.52	8655.12	8429.96	8071.03	7632.76
Distributionally robust optimization/$	7699.94	7327.65	7001.95	6800.40	6760.25

The trend of the pre-scheduling cost of DRO changing with the mean value is the same as that of stochastic optimization, indicating that it has the characteristic of reflecting risk expectation as stochastic optimization. Its higher pre-scheduling cost indicates that it has the robustness as robust optimization.

6. Conclusions

In order to effectively address the uncertainty risks of port energy system caused by intermittence and fluctuation of renewable energy, this paper proposes a scheduling method for port energy system based on distributionally robust optimization (DRO). This method organically integrates Wasserstein distance-based fuzzy set, "electricity, green hydrogen, ammonia synthesis", and distributionally robust optimization, and uses ammonia synthesis after hydrogen production by water electrolysis (P2H2A) as a flexible resource to improve the capacity of renewable energy utilization, which helps to achieve optimal scheduling of the port energy system. Finally, based on the real data of port energy system, example analysis was conducted, and the following conclusions were obtained.

(1) The time series scheduling model of P2H2A is intuitive to quantify the capacity for adjust the speed of the change of load rate. P2H2A can provide low-carbon flexible resources for the port energy system, has the ability to adapt to the uncertainty of renewable energy, and can effectively improve the economy of the port energy system scheduling scheme.
(2) The scheduling method based on DRO, which realizes combined operation of day-ahead stage and intraday stage, overcomes the shortcomings as the poor risk-resistance of stochastic optimization and too conservative of robust optimization. It can simultaneously have the advantages as stochastic optimization reflecting risk expectation based on historical prediction error data and robust optimization with strong robustness.
(3) Wasserstein distance-based fuzzy set is used to characterize the uncertainty of renewable energy power generation. Under the two risk preferences of risk neutral and risk averse, DRO can balance the economy and robustness of scheduling schemes by flexibly adjusting the Wasserstein distance-based sphere radius. It helps the port energy system consider the uncertainty of renewable energy generation to balance the economy and robustness of scheduling schemes.

In order to further improve the real-time and practical performance of scheduling method, the next research focus will be on exploring the construction of a multiple time scales collaborative scheduling framework considering the uncertainty of load, which integrates DRO, rolling optimization of intraday stage, and real-time compensation mechanisms.

Data availability

The data that support the findings of this study are available from the corresponding author upon reasonable request.

Ethical statement

Ethics approval was not required for this research.

CRediT authorship contribution statement

Xiaoou Liu: Writing – review & editing, Writing – original draft, Visualization, Validation, Supervision, Software, Resources, Project administration, Methodology, Investigation, Funding acquisition, Formal analysis, Data curation, Conceptualization.

Declaration of competing interest

The authors declare that they have no known competing financial interests or personal relationships that could have appeared to influence the work reported in this paper.

References

[1] United Nations Conference on Trade and Development, Review of Maritime Transport 2021[R], United Nations, Geneva, 2021.
[2] IRIS Ç, J.S.L. Lam, A review of energy efficiency in ports: operational strategies, technologies and energy management systems, Renew. Sustain. Energy Rev. 112 (2019) 170–182.
[3] Yue Zhang, Chengji Liang, Jian Shi, Gino Lim, Yiwei Wu, Optimal port microgrid scheduling Incorporating onshore power supply and berth allocation under uncertainty, Appl. Energy 313 (2022) 118856.
[4] Shuai Yang, Jun Yuan, V. Nian, et al., Economics of marinised offshore charging stations for electrifying the maritime sector, Appl. Energy (2022) 322.
[5] Panda, Nihar Ranjan, et al., Enhanced hydrogen generation efficiency of methanol using dielectric barrier discharge plasma methodology and conducting sea water as an electrode, Heliyon 6 (9) (2020) e04717.
[6] D.R. MacFarlane, P.V. Cherepanov, J. Choi, et al., A roadmap to the ammonia economy, Joule 4 (6) (2020) 1186–1205.
[7] J. Incer-Valverde, L.J. Patiño-Arévalo, G. Tsatsaronis, et al., Hydrogen-driven Power-to-X: state of the art and multicriteria evaluation of a study case, Energy Convers. Manag. 266 (2022) 115814.
[8] E. Vichos, N. Sifakis, T. Tsoutsos, Challenges of integrating hydrogen energy storage systems into nearly zero-energy ports, Energy (2022) 241.
[9] Ashish M. Gujarathi, et al., Towards technology, economy, energy and environment oriented simultaneous optimization of ammonia production process: further analysis of green process, Heliyon 9 (11) (2022) e21802.

[10] J. Li, J. Lin, P.M. Heuser, et al., Co-planning of regional wind resources-based ammonia industry and the electric network: a case study of Inner Mongolia, IEEE Trans. Power Syst. 37 (1) (2022) 65–80.
[11] Rony Escobar-Yonoff, Daniel Maestre-Cambronel, Sebastián Charry, Adriana Rincón-Montenegro, Ivan Portnoy, Performance assessment and economic perspectives of integrated PEM fuel cell and PEM electrolyzer for electric power generation, Heliyon 7 (3) (2021) e06506.
[12] Wei Liu, Yanming Wan, Yalin Xiong, et al., Key technology of water electrolysis and levelized cost of hydrogen analysis under carbon neutral vision, Trans. China Electrotech. Soc. 37 (11) (2022) 2888–2896.
[13] B. Daria, E. Yassine, F. Giulio, et al., A Bi-level optimization-based architecture for the scheduling and real-time control of microgrids with hydrogen production system, IFAC-PapersOnLine 56 (2) (2023) 8284–8289.
[14] Ercan Aykut, Bahtiyar Dursun, Sertaç Görgülü. Comprehensive environmental and techno-economic feasibility assessment of biomass- solar on grid hybrid power generation system for Burdur Mehmet Akif Ersoy University Istiklal Campus. Heliyon, 9(11): e22264.
[15] S.S. Beerbühl, M. Fröhling, F. Schultmann, Combined scheduling and capacity planning of electricity-based ammonia production to integrate renewable energies, Eur. J. Oper. Res. 241 (3) (2015) 851–862.
[16] A. Allman, P. Daoutidis, Optimal scheduling for wind powered ammonia generation: effects of key design parameters, Chem. Eng. Res. Des. 131 (2018) 5–15.
[17] S. Klyapovskiy, Y. Zheng, S. You, et al., Optimal operation of the hydrogen-based energy management system with P2X demand response and ammonia plant, Appl. Energy 304 (2021) 117559.
[18] Xiaodong Zheng, Yan Xu, Zhengmao Li, Haoyong Chen, Co-optimisation and settlement of power-gas coupled system in day-ahead market under multiple uncertainties, IET Renew. Power Gener. 15 (34) (2021) 1632–1647.
[19] Bilal Abu-Salih, Pornpit Wongthongtham, Greg Morrison, Kevin Coutinho, Manaf Al-Okaily, Ammar Huneiti, Short-term renewable energy consumption and generation forecasting: a case study of Western Australia, Heliyon 8 (3) (2022) e09152.
[20] F.F. Shen, L. Zhao, W.L. Du, et al., Large-scale industrial energy systems optimization under uncertainty: a data-driven robust optimization approach, Appl. Energy 259 (2020) 114199.
[21] Bo Zhou, Xiaomeng Ai, Jiakun Fang, et al., Continuous-time modeling based robust unit commitment considering beyond-the-resolution wind power uncertainty, Trans. China Electrotech. Soc. 36 (7) (2021) 1456–1467.
[22] Miao Wang, Zhuopeng Shi, Wei Luo, Yi Sui, Dongxun Wu, Distributionally robust optimal scheduling of integrated energy systems including hydrogen fuel cells considering uncertainties, Energy Rep. 10 (29) (2023) 1575–1588.
[23] Y. Chen, W. Wei, F. Liu, et al., Distributionally robust hydro-thermal-wind economic dispatch, Appl. Energy 173 (2016) 511–519.
[24] F. Alismail, P. Xiong, C. Singh, Optimal wind farm allocation in multi-area power systems using distributionally robust optimization approach, IEEE Trans. Power Syst. 33 (1) (2018) 536–544.
[25] Hongxu Huang, Rui Liang, Chaoxian Lv, et al., Two stage robust stochastic scheduling for energy recovery in coal mine integrated energy system, Appl. Energy (2021) 290.
[26] Yongsheng Cao, Demin Li, Yihong Zhang, et al., Optimal energy management for multi-microgrid under a transactive energy framework with distributionally robust optimization, IEEE Trans. Smart Grid 13 (1) (2021) 599–612.
[27] H. Ishaq, I. Dincer, Dynamic modelling of a solar hydrogen system for power and ammonia production, Int. J. Hydrogen Energy 46 (27) (2021) 13985–14004.
[28] Y. Qiu, B. Zhou, T. Zang, et al., Extended Load Flexibility of Industrial P2H Plants: A Process Constraint-Aware Scheduling Approach [C], IEEE 5th International Electrical Energy Conference, Nanjing, China, 2022.
[29] G. Sakas, A. Ibáñez-Rioja, V. Ruuskanen, et al., Dynamic energy and mass balance model for an industrial alkaline water electrolyzer plant process, Int. J. Hydrogen Energy 47 (7) (2022) 4328–4345.
[30] K. Verleysen, A. Parente, F. Contino, How sensitive is adynamic ammonia synthesis process? Global sensitivity analysis of a dynamic Haber-Bosch process, Energy 232 (2021) 121016.
[31] J. Li, J. Lin, Y. Song, Capacity Optimization of Hydrogen Buffer Tanks in Renewable Power to Ammonia (P2A) system[C], IEEE Power & Energy Society General Meeting (PESGM), Montreal, 2020. Canada.
[32] R.J. Zhu, H. Wei, X.Q. Bai, Wasserstein metric based distributionally robust approximate framework for unit commitment, IEEE Trans. Power Syst. 34 (4) (2019) 2991–3001.
[33] G.C. Pflug, D. Wozabal, Ambiguity in portfolio selection, Quant. Financ. 7 (2007) 435–442.
[34] P. Xiong, P. Jirutitijaroen, C. Singh, A distributionally robust optimization model for unit commitment considering uncertain wind power generation, IEEE Trans. Power Syst. 32 (1) (2017) 39–49.
[35] C. Duan, W.L. Fang, L. Jiang, et al., Distributionally robust chance-constrained approximate AC-OPF with Wasserstein metric, IEEE Trans. Power Syst. 33 (5) (2018) 4924–4936.
[36] Y.W. Wang, Y.J. Yang, L. Tang, et al., A Wasserstein based two-stage distributionally robust optimization model for optimal operation of CCHP micro-grid under uncertainties, Int. J. Electr. Power Energy Syst. 119 (2020) 105941.
[37] C. Zhao, Y. Guan, Data-driven risk-averse stochastic optimization with Wasserstein metric, Oper. Res. Lett. 46 (2) (2018) 262–267.
[38] Tennet. System, Transmission Data [EB/OL, 2022-10-27 [2022-10-27], https://www.tennet.org.